CHAPTER 7

RESULTS ON ELETRICAL IMPEDANCE SPECTROSCOPY OF POLY(ε -CAPROLACTONE) COMPLEXES

7.1 Introduction

The composition dependence of the impedance analysis will be studied at room temperature. From the impedance plot, an appropriate equivalent circuit model will be used to fit the experimental data. The bulk resistance value of the sample will then be extracted and applied in an equation to calculate the dc conductivity. From DSC, XRD and FTIR studies in chapter 4, 5 and 6, the lowest relative degree of crystallinity and the highest free ion integral area percentage are obtained for the sample containing 26 wt.% salt and 50 wt.% EC for PCL-NH_4SCN and PCL-NH_4SCN-EC systems, respectively. Therefore, the highest conductivity is expected to occur for the respective sample which will be verified in this study. Temperature dependence studies at selected compositions will also be carried out. The conductivity-temperature relationship will be explained using the most relevant model.

The dielectric behavior of PCL-NH_4SCN and PCL-NH_4SCN-EC systems will be analyzed in detail. The effect of NH_4SCN and EC concentration on dielectric properties as a function of frequency will be investigated. These dielectric properties include the complex relative permittivity, complex electric modulus, loss tangent and complex conductivity. The outcome of the study should shed some light on the ion transport properties of both systems.

7.2 Electrical studies of PCL-NH_4SCN system

7.2.1 Composition Dependence of Conductivity

Fig. 7.1 depicts the impedance plot of PCL incorporated with different concentrations of NH_4SCN at room temperature.

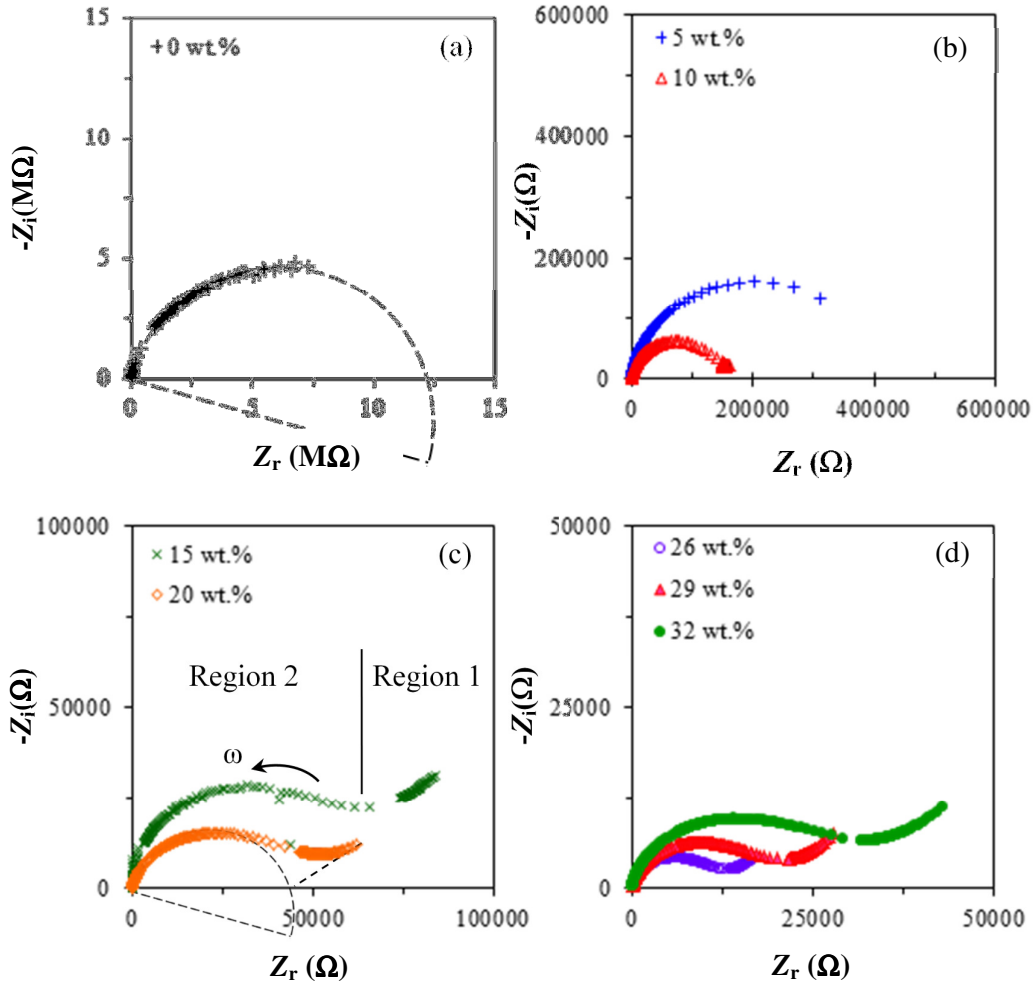

Fig. 7.1. Impedance plot for PCL-NH_4SCN films added with 0 to 32 wt.% NH_4SCN at room temperature.

Fig. 7.1(a) is the Nyquist plot of pure PCL (0 wt.% salt) showing a depressed semicircle making an intersection with real axis at 12.5 MΩ. This semicircle is depressed with the center below the real axis. It is attributed to the distribution of relaxation times of the bulk electrolyte [Macdonald, 1987] and reveals the non-Debye nature of the material.

For samples containing 5 wt.% and 10 wt.% NH_4SCN in Fig. 7.1(b), smaller depressed semicircles are observed but intersect with real axis at much lower resistance value, 0.41 and 0.15 MΩ respectively. As the salt content increases to 15 wt.% onwards, two well defined regions can be observed in Fig. 7.1(c) and (d). An inclined spike at the low frequency region and a depressed semicircle at high frequency region. According to Kim *et al*. (1999), the inclined spike should be parallel to the imaginary axis but polarization effect at electrode/electrolyte interface causes the inclination. This polarization effect is the result of the double layer at the blocking electrodes [Song *et al*., 2000].

The experimental data of impedance can be fitted by an idealized equivalent circuit model composed of discrete electrical components. This circuit consists of a resistor, *R* and two non-ideal bulk geometrical capacitors known as a constant phase element, *CPE*. The impedance of each *CPE*, Z_{CPE} can in general be expressed by:

$$Z_{CPE} = k(j\omega)^{-p} \tag{7.1}$$

where k is CPE coefficient and p is a dimensionless experimental parameter between zero and unity [MacDonald, 1987]. When p = 1, the CPE would become identical to a capacitor with inverse of k corresponding to the capacitance, C value and $Z_C = (j\omega C)^{-1}$.

The fitting is done by modeling a parallel combination of a resistor (representing the mobile ions inside the polymer matrix) and CPE 1 (representing the immobile polymer chain) in series with another CPE 2 circuit network. The capacitance value of the parallel CPE 1 is usually of the order of nano-Farads [Nadeem *et al.*, 2002].

Fig. 7.2 shows the fitting of the equivalent circuit to the experimental data of PCL incorporated with 26 wt.% NH_4SCN. The fitted data plot is shown as the solid line while the experimental data is presented as the triangle marker.

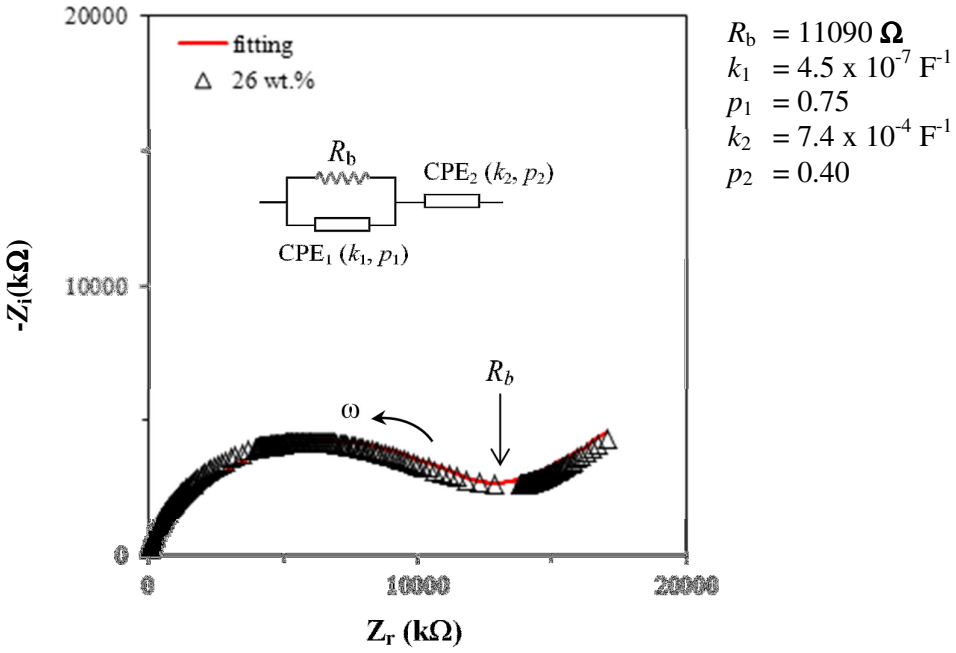

Fig. 7.2. Fitting of the equivalent circuit to the experimental data of PCL-NH_4SCN films added with 26 wt.% NH_4SCN.

It can be seen that the fitted data matches well the experimental data. The extracted parameters such as k_1, p_1, R_b, k_2 and p_2 are obtained to be 4.5×10^7 F^{-1}, 0.75, 11090 Ω, 7.4×10^4 F^{-1} and 0.40, respectively.

The electrical conductivity is then obtained using the following relation:

$$\sigma = \frac{d}{R_B A} \tag{7.2}$$

where σ is the dc conductivity, d is the thickness of the electrolyte sample, A is the surface area of sample-electrode contact and R_B is the bulk electrolyte resistance. R_B could be obtained from the fitting process or simply taking the semicircle intercept with the spike and extrapolating it downwards to the horizontal axis. The room temperature conductivity as a function of salt content is depicted in Fig. 7.3.

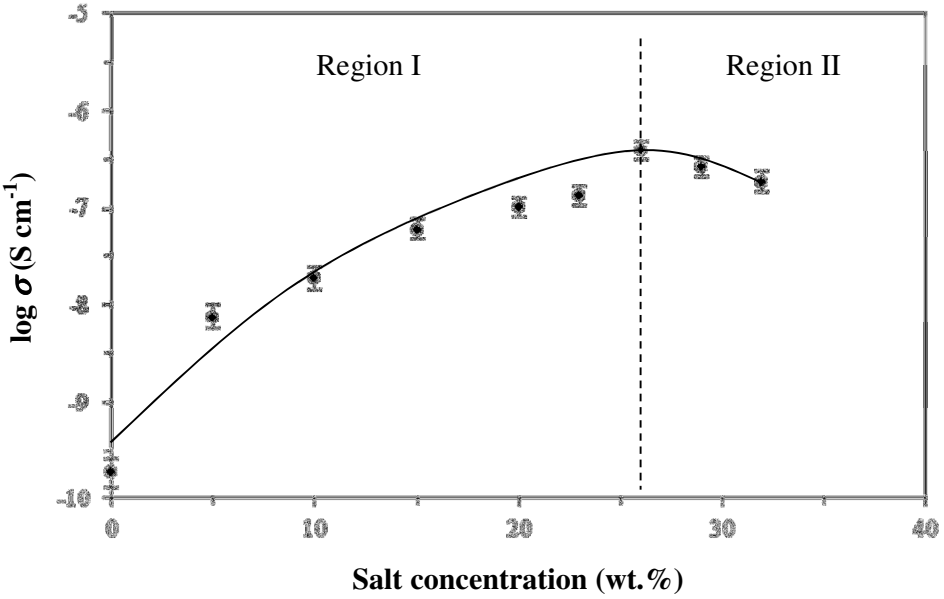

Fig. 7.3. Salt concentration dependence of dc conductivity at room temperature. The line is just a guide to the eye.

The conductivity of pure unsalted PCL obtained in Fig. 7.3 at room temperature is 1.86 x 10^{-10} S cm^{-1}. This value is of the same order of magnitude as obtained by Hirai *et al.* (2007). When 5 and 10 wt.% of NH_4SCN is added to the PCL film, the conductivity of the PCL-NH_4SCN film increases to 7.45 x 10^{-9} S cm^{-1} and 1.85 x 10^{-8} S cm^{-1}, respectively. It can be seen that the conductivity continues to increase with increasing salt content, reaching a maximum value of 3.94 x 10^{-7} S cm^{-1} at 26 wt.% salt content (Region I).

This conductivity value is comparable to other PCL-salt systems as reported in the literature, which are 1 x 10^{-7} S cm^{-1} for (PCL-siloxane)-KCF_3SO_3 (80:20) system [Fernandes *et al.*, 2011a], 1.5 x 10^{-7} S cm^{-1} for PCL-PC-$LiBF_4$ (78:10:12) system [Fonseca *et al.*, 2007], 6 x 10^{-7} S cm^{-1} for (MPEG-PCL)-$LiClO_4$ (75:25) system [Chiu *et al.*, 2005] and 6.3 x 10^{-7} S cm^{-1} for PEO-PCL-$LiClO_4$ (60:15:25) system [Chiu *et al.*, 2004], respectively. This indicates that the present PCL-NH_4SCN system can host ionic conduction as good as other polymeric materials. At higher salt concentration in Region II, 29 and 32 wt.%, the conductivity begins to fall to 2.57 x 10^{-7} S cm^{-1} and 1.86 x 10^{-7} S cm^{-1} respectively.

7.2.2 Composition Dependence of Dielectric Behavior

In most of the application in electrochemical devices, dielectric behavior plays an essential role to determine the potential or usefulness of the devices. The dielectric study in polymer electrolyte system helps to understand the polarization effect, ionic conduction behavior and could correlate the relaxation time with ionic conductivity.

Therefore, a detailed study on the dielectric properties of PCL-NH_4SCN samples is essential. The room temperature (RT) frequency dependence of dielectric properties at various salt concentrations for PCL-NH_4SCN polymer electrolytes is investigated.

Complex relative permittivity has a real component, ε' and an imaginary component, ε''. ε' measures the ability of a material to polarise the amount of dipole alignment in a given volume and corelate with capacity to store electric charge [Sheha, 2009]. ε'' is a measure of energy losses to align dipoles or/and move electric charges due to the polarity changes of electric field and is also associated to the material's conductivity. Fig. 7.4 depicts the variation of log ε' versus log f for PCL- NH_4SCN films added with 0 to 32 wt.% NH_4SCN at RT. Log scale is used for y-axis in order to observe the variation of ε' clearly with increasing salt content at high frequency region.

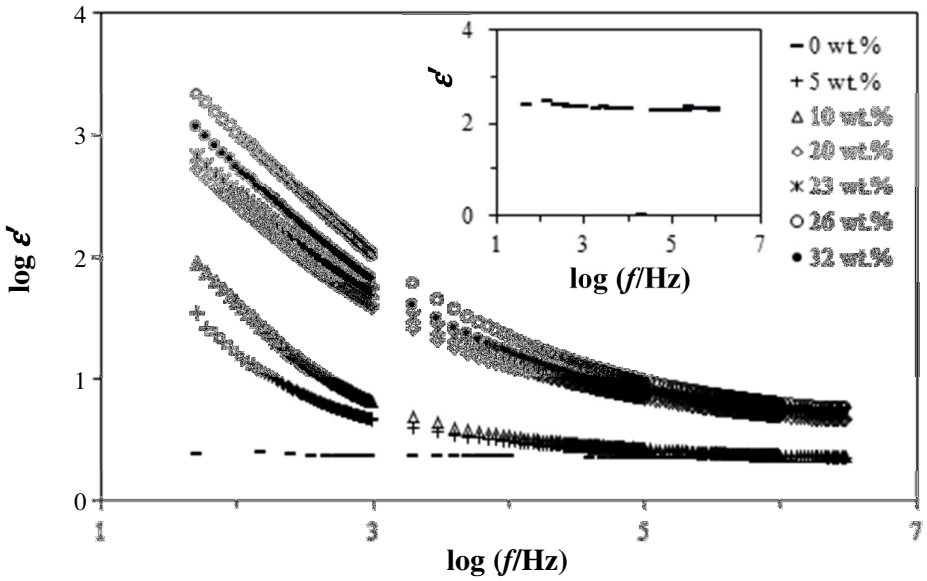

Fig. 7.4. Variation of log ε' versus log f for PCL-NH_4SCN films added with 0 to 32 wt.% NH_4SCN at room temperature. Inset displays the ε' versus log f for 0 wt.% salt.

At low frequency region, a dispersion with high value of ε' is observed which can be attributed to electrode polarization effect. The value of ε' for PCL-salt complexes is high, in the range of ~10^3 at low frequency region compared to 2.9 of pure PCL film [Lince *et al*., 2008]. The present study gave a value of 2.3 for PCL film with 0 wt.% salt as shown in Fig. 7.4 inset. Many other polymer-salt systems revealed similar polarization effect such as PEO-based systems [Sengwa and Sankhla, 2008; Pradhan, 2009]. At high frequency region, ε' is seen to decrease rapidly.

An important characteristic of any electrolyte, in relation to the conductivity is the number of charge carriers. In polymer electrolytes, the charge carriers are ions and its number density depends upon both the dissociation energy U involved and ε' according to equation 7.4 [Awadhia and Agrawal, 2007; Ramya *et al*., 2008]:

$$n = n_0 \exp(-U / \varepsilon' kT) \tag{7.4}$$

Here, k is the Boltzmann constant. Referring to the above equation, an increase in ε' would reflect an increase in n. From Fig. 7.4, the variation of ε' with salt content seems to follow the variation of conductivity. Therefore, ε' as a function of salt content is plotted to explain the conductivity phenomena from the angle of number density of charge carriers. Salt concentration dependence of ε' at 0.3 kHz, 3 kHz, 30 kHz and 1 MHz is plotted in Fig. 7.5.

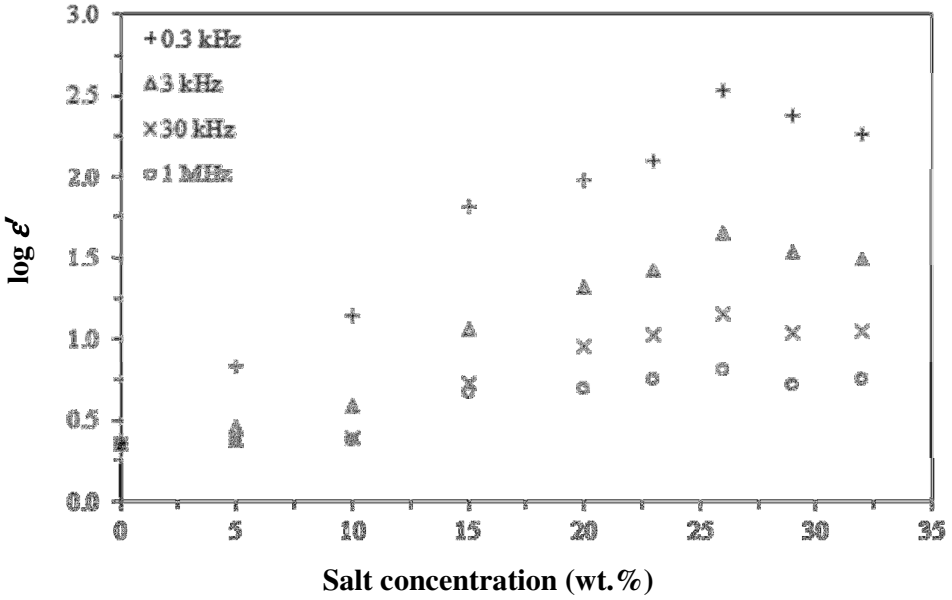

Fig. 7.5. Salt concentration dependence of real relative permittivity for PCL-NH_4SCN films at selected frequencies.

Fig. 7.5 is for comparison to Fig. 7.3. The variation of ε' as a function of salt concentration is clearly following the same trend as conductivity variation with salt concentration. ε' increases with increasing salt content until 26 wt.%. The highest conducting sample in conductivity study has the highest value of ε' at 26 wt.%. According to equation 7.4, this implies that the number density of charge carriers have increased with addition of salt content. Since the charge is due to ions, increase in charge is a proof of increase in the number density of ions and hence explains the increase in conductivity at room temperature.

The reduction in ε' at 26 wt.% onwards can be attributed to the decreasing number density of free ions. In other words, the conductivity could be possibly tuned by the ε' value of the polymer electrolyte system. It is good to note that the ε' value is determined by the injecting salt content. By plotting σ as a function of ε' at selected frequencies, as depicted by Fig. 7.6, a correlation between σ and ε' can be better

observed. A few frequencies are selected to represent the wide frequency range of this study.

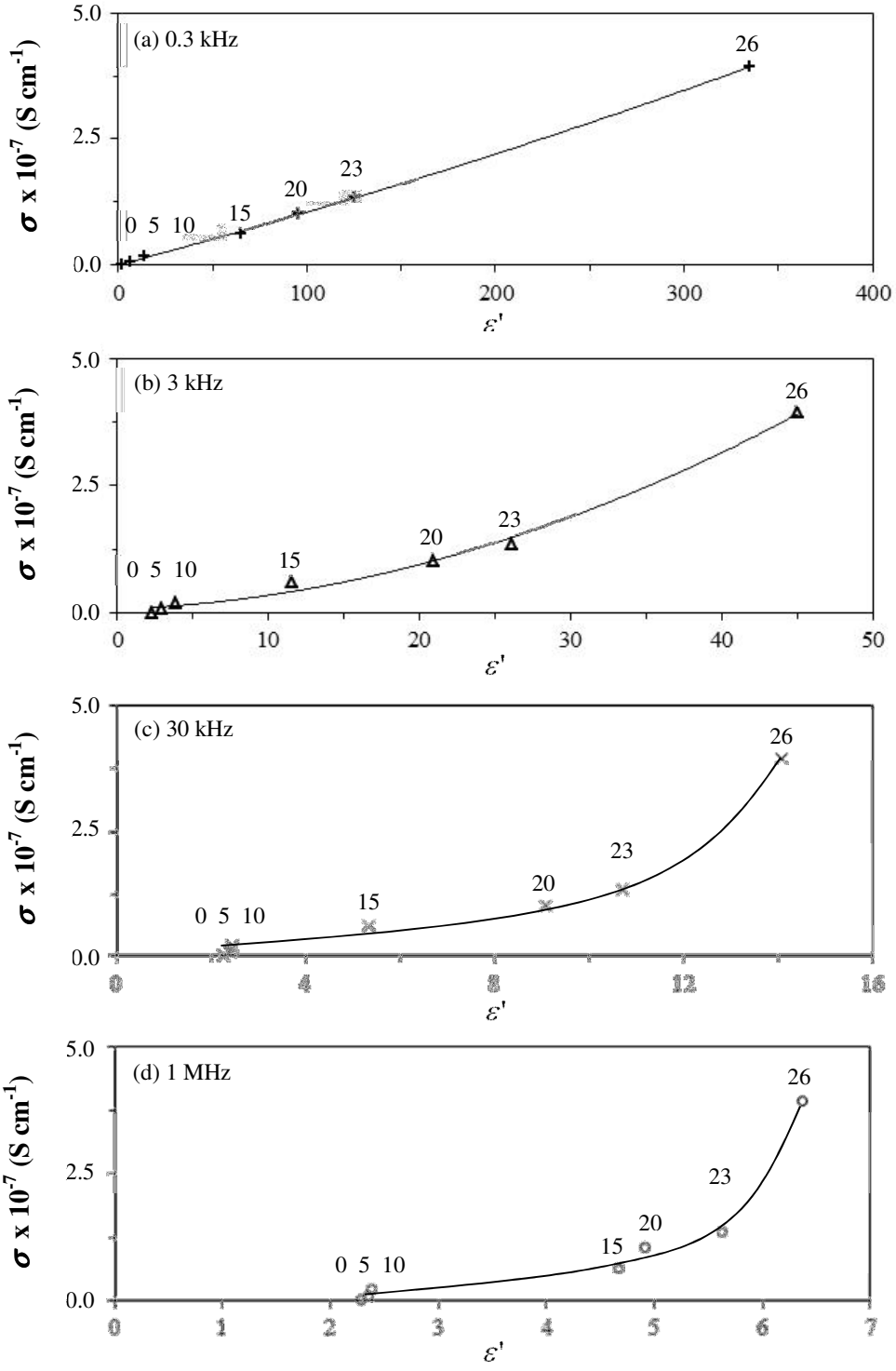

Fig. 7.6. Conductivity as a function of real relative permittivity at selected frequencies. Salt concentrations in wt.% are labeled within the figures.

Fig. 7.6 reveals a possible strong dependence of conductivity on ε' value of the PCL-NH_4SCN polymer electrolyte system. This empirical description for the correlation between σ and ε' has been known in organic liquid electrolyte system. In all the liquid systems using tetrabutylammonium triflate, lithium triflate or lithium iodide [Petrowsky and Frech, 2009)] as salt and alcohol [Petrowsky and Frech, 2008; Fleshman, *et al*., 2011], alkly bromide, nitrile or acetate [Bopege *et al*., 2012] as solvent, Petrowsky and co-workers have proposed a new Arrhenius formalism. Instead of $\sigma_{dc}(T) = \sigma_o\, e^{-E_a/K_BT}$ where σ_{dc} is the temperature dependent dc counductivity and σ_o is a constant, the researchers proposed $\sigma_{dc}(T, \varepsilon') = \sigma_o(\varepsilon')\, e^{-E_a/K_BT}$. In the new Arrhenius formalism, σ_{dc} depends on both parameters of T and ε' where ε' is contained in σ_o .

ε'' versus log *f* plot is presented in Fig. 7.7. Log scale is used for y-axis in order to observe the small magnitude of dielectric loss peak, if any [Jayathilaka *et al*., 2003].

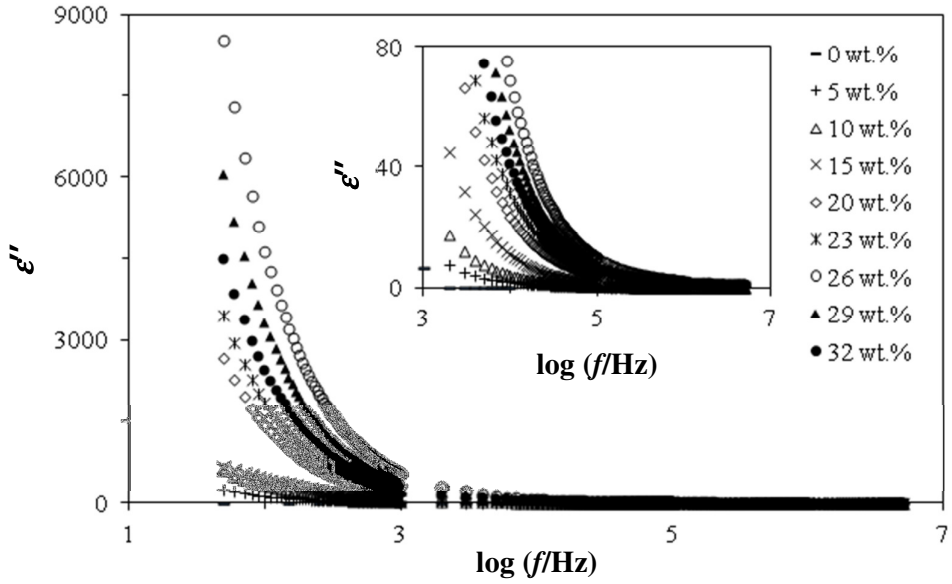

Fig. 7.7. Variation of ε'' versus log *f* for PCL-NH_4SCN films added with 0 to 32 wt.% NH_4SCN at room temperature. Inset displays the magnified graph.

Similar observation as ε' is depicted, the high value of ε'' at low frequency is due to electrode polarization effect. As frequency increases, ε'' decreases drastically. The variation of ε'' with increasing salt content is also very much similar as in conductivity-salt relationship in Fig.7.3.

There is no dielectric loss peak observed within the frequency window in this study. This is unexpected because Baysal and Stockmayer (1994) reported a dielectric loss peak at around 60 kHz for a dilute solution of PCL in dioxane at 298 K. They termed it as normal mode dipolar relaxation because the dipole moment is parallel to the main polymer chain. However, the peak magnitude is very small, around 0.2. For semidilute solution of PCL in benzene at 298 K, a similar dielectric loss peak was also reported with peak magnitude below 1.0 [Urakawa *et al.*, 1994].

Dipolar relaxation is defined as the time delay for the dipole to recover to its unperturbed state upon removal of electric field. It behaves like a resonance effect in an oscillator. In principle, a dipolar relaxation peak is expected to appear if the frequency of the applied electric field is the same as the natural frequency of the dipoles [Tiller, 1992]. In polymer electrolyte system, dipolar relaxation is the manifestation of polymer segmental motion.

For the present study, this dipolar relaxation peak could possibly be masked by the overwhelmingly large electrode polarization effect ($\varepsilon''_{elec} >> \varepsilon''_{relax}$). ε''_{elec} and ε''_{relax} represents the dielectric loss due to electrode polarization and dipolar relaxation, respectively. Thus, it is difficult to study the relaxation behavior in ionic conducting

materials using the traditional dielectric analysis. Instead, electric modulus analysis is attempted as alternative to study the relaxation dynamics.

Electric modulus is useful to study ionic transport dynamics but it is a topic to debate since its inception in the 80s [Ngai and Rendell, 2000; Sidebottom *et al*., 2000; Hodge *et al*., 2005; Macdonald, 2009]. Nonetheless, the fitting function of electric modulus to the experimental data is successful from low frequency region up to 10 f_m [Sidebottom *et al*., 2000]. f_m represents the frequency of the peak. Electric modulus is particularly useful to analyze electrical relaxation processes because it is defined as the reciprocal of complex relative permittivity. Since ε' contributes as the denominator to the second power in the loss function, the inversion process is able to suppress the electrode polarization effect at low frequencies and enhance small features at high frequencies [Starkweather and Avakian, 1992]. Fig.7.8 depicts the real parts of electric modulus versus log f for PCL-NH_4SCN films added with 0 to 32 wt.% NH_4SCN at room temperature.

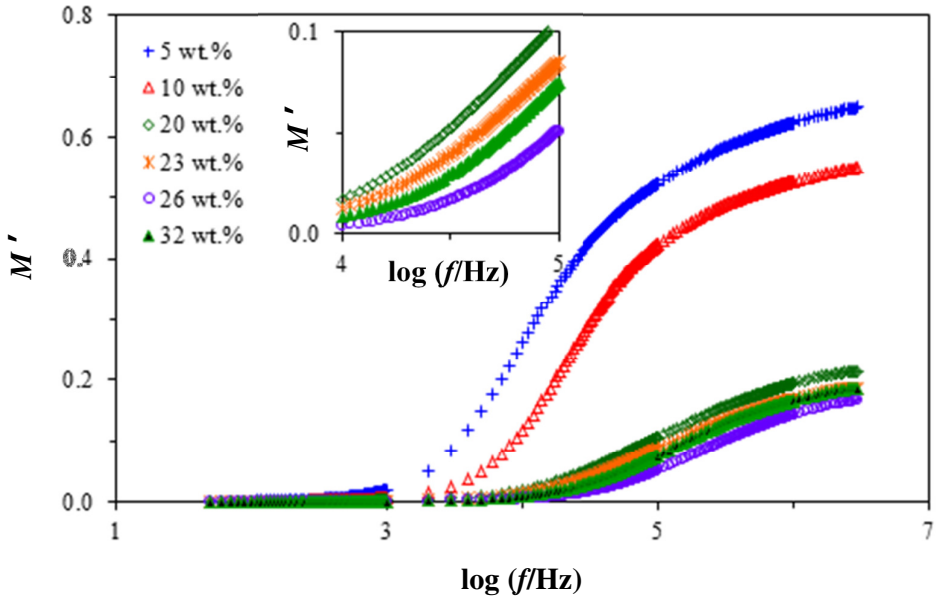

Fig. 7.8. Variation of M' versus log f for PCL- NH_4SCN films added with 0 to 32 wt.% NH_4SCN at room temperature. Inset shows the magnified graph.

At low frequency region, it can be observed in Fig.7.8 that M' approaches zero and this tail is attributed to the large capacitance associated with the electrode polarization [Gogulamurali *et al*., 1992]. At high frequency region, M' shows a sigmoidal shape for all samples as expected. As more salt is added, M' decreases as the sigmoidal spectra shift to the right, opposite to that of relative permittivity. It is good to note that the variation of the spectra follows the trend like conductivity with salt content.

Fig. 7.9 presents the imaginary parts of electric modulus versus log *f*.

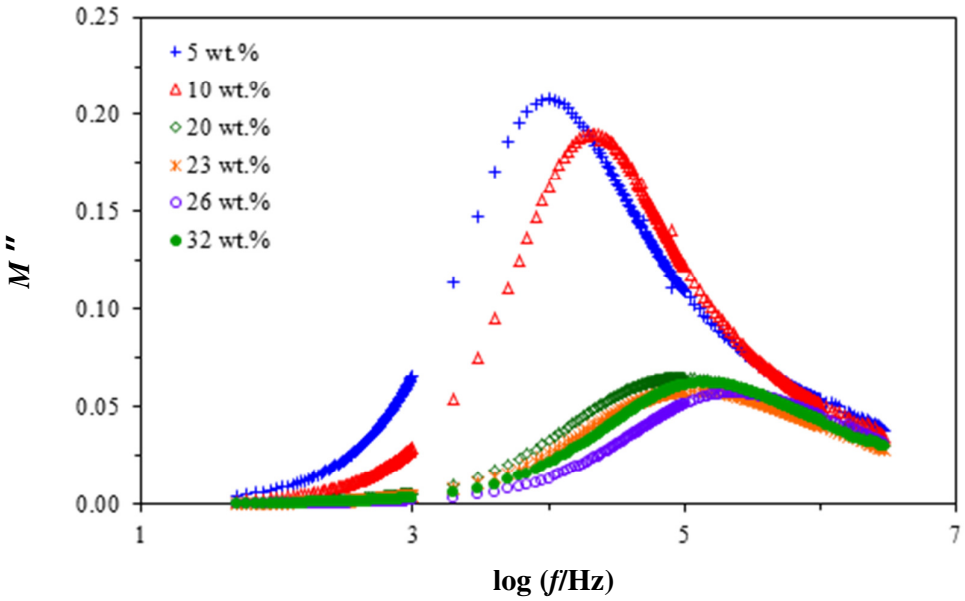

Fig. 7.9. Variation of M'' versus log *f* for PCL-NH_4SCN films added with 0 to 32 wt.% NH_4SCN at room temperature.

Fig. 7.9 displays a single, broad and asymmetric M'' peak for all samples. For 5 wt.% salt, the M'' peak is depicted at 10 kHz. As salt concentration increases, this peak is observed to shift to higher frequency, indicating shorter relaxation time. The variation of the peaks also follow the conductivity trend with salt content. According to Pradhan

et al. (2009), a single well defined resonance peak is an indication of long range conductivity relaxation due to ionic motion.

The conductivity relaxation can be explained as follows. An ion may have more than one equilibrium site of equal potential energies and be separated by a potential barrier. This ion may hop to the adjacent site with the natural jump frequency [Druger *et al*., 1985]. When the frequency of the external field is comparable to the natural frequency, maximum energy is transferred resulting in resonance effect.

However, the M'' peak is quite broad and the full width at half maximum (FWHM) is greater than 1.144 decades displaying a stretched exponential function. This means that M'' exhibits a non-Debye behaviour and does not indicate conductivity relaxation. Instead, it can be intepreted as the dipolar relaxation that exhibit a distribution of relaxations time. Furthermore, the existence of dipolar relaxation of PCL was supported by other researchers [Baysal and Stockmayer, 1994; Urakawa *et al*., 1994]. They captured the dipolar relaxation peak at around 60 kHz (for pure PCL sample) and attributed to the polymer chain entanglement. Thus, a way must be found to verify the type of M'' relaxation peak represents, whether conductivity relaxation or dipolar relaxation.

A useful method was proposed by Moynihan and co-workers [Ambrus *et al*., 1972; Macedo *et al*., 1972] to compare M'' and ε'' simultaneously. Referring to Fig. 7.9 and Fig. 7.7, a relaxation peak in M'' and a dispersion (no peak) in the corresponding ε'' is observed. They suggested that such analysis would conclude that the M'' peak represents the conductivity relaxation. Another group of researchers, Mohomed *et al*. (2005) suggested to plot M'' versus M'. According to the researchers,

a complete and true semicircle arc shows the conductivity relaxation while a non-semicircle plot deny the conductivity relaxaton. Therefore, the argand plot of M'' versus M' is plotted in Fig. 7.10.

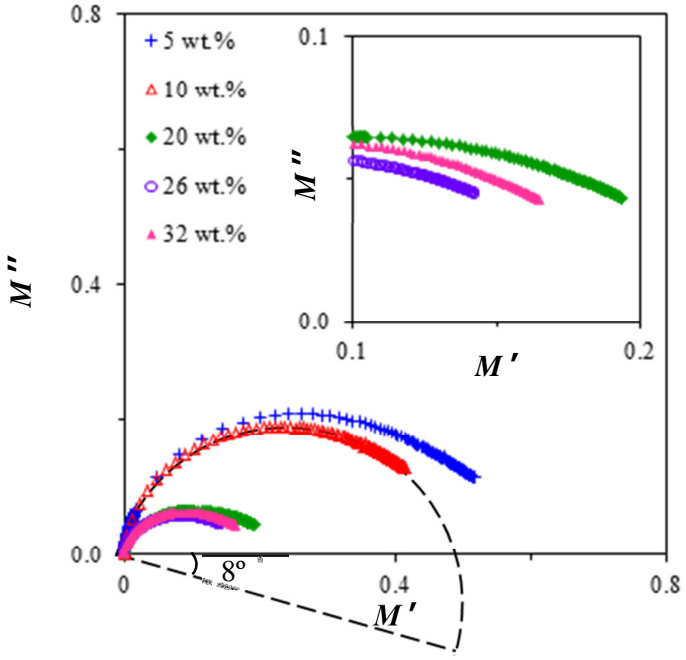

Fig. 7.10. Argand plot of M'' versus M' for PCL-NH_4SCN films added with 0 to 32 wt.% NH_4SCN. Inset shows the magnified graph.

Fig. 7.10 shows a semicircle arc but tilted at 8º to the horizontal axis that passes through the origin. This depressed semicircle indicates a combination of both conductivity and dipolar relaxations [Starkweather and Avakian, 1992]. This coupling was reported in the literature. PEO-sodium salt system reported by Jeevanandam and Vasudevan (1998) has shown a single peak in the loss modulus spectra and a simple dispersion in the dielectric loss spectra, leading to the conclusion that the ionic motion is coupled to the polymer segmental motion. In another system of poly(propylene glycol) (PPG) complexed with lithium salt [Fu *et al.*, 1991], at very low temperature and low salt content, M'' displayed two separate relaxation peaks initially. As the salt

concentration was increasing, the two peaks was observed to get closer to one another. Until a certain salt content with ether oxygen to lithium ratio 30:1, the two peaks merged indicating a coupling between ion motion and polymer segmental motion. In the present work, since the operating temperature (25 ºC) of PCL-NH_4SCN complex is well above T_g (-60 ºC), therefore the ionic motion is most probably assisted by the polymer segmental motion. The coupling motions will be further studied when temperature dependence is considered.

The loss tangent, tan δ, was analyzed to observe the relaxation behavior in the polymer electrolytes. tan δ can be obtained from the ratio of real impedance to imaginary impedance. It is also the ratio of energy loss to energy stored and called dissipation factor. The variation of loss tangent as a function of frequency for PCL-NH_4SCN films added with 0 to 32 wt.% NH_4SCN is presented in Fig. 7.11.

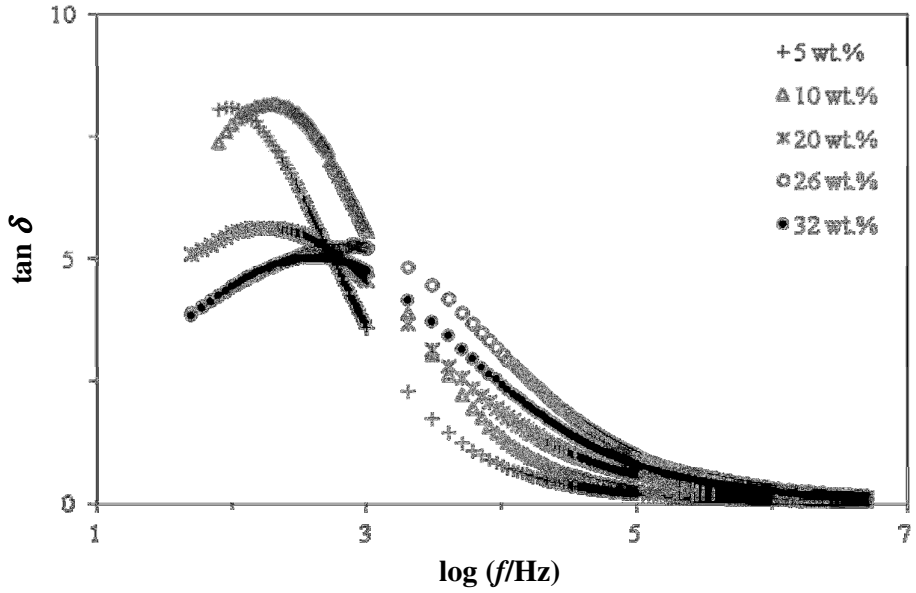

Fig.7.11. Variation of loss tangent versus log *f* for PCL-NH_4SCN films added with 0 to 32 wt.% NH_4SCN at room temperature.

The loss tangent consists of a well-defined peak at a characteristic frequency. When the real impedance is more dominant than the imaginary impedance at low

frequency region, tan δ increases with frequency. As frequency increases, the imaginary impedance grows in proportion to the frequency [Chopra *et al*., 2003] but the real impedance decreases gradually with frequency. Eventually, the imaginary impedance exceeds the real impedance, showing a peak at a characteristic frequency.

The loss peak is seen to shift towards the higher frequency with increasing salt content. This means a decreasing relaxation time. By taking Debye equation in an ideal case, the relaxation time, τ can be calculated from the characteristic frequency of the peak, f_m according to:

$$\omega \cdot \tau = 2\pi f_m \cdot \tau = 1 \tag{7.1}$$

The relaxation time is plotted in Fig. 7.12 as a function of salt concentration at room temperature.

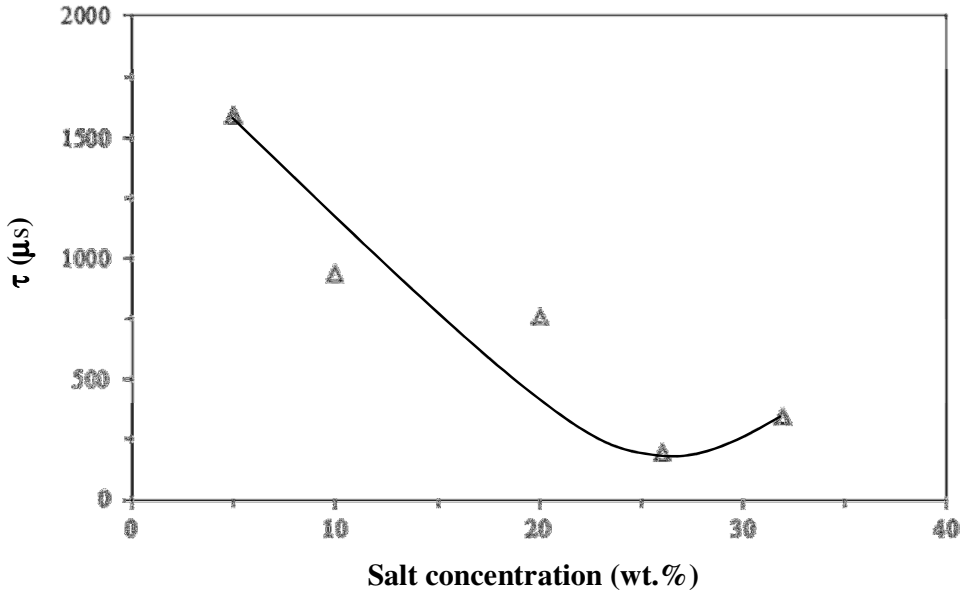

Fig. 7.12. Salt concentration dependence of relaxation time at room temperature. The line is just a guide to the eye.

Fig. 7.12 clearly shows that the variation of relaxation time is the inverse of dc conductivity variation as depicted in Fig. 7.3. The dc conductivity is increasing with the salt content until a maximum at 26 wt.% while the relaxation time is reducing until a minimum at the same salt concentration. As more salt is incorporated, the amorphous region expands and molecular packing becomes loose and weak. Polymer chain is now more flexible to orient, resulting in a reduction of relaxation time. The shortest relaxation time is recorded for the most conducting sample [Singh and Gupta, 1998].

The real part of complex conductivity, σ' as presented in Fig. 7.13, can also be used to estimate the dc conductivity obtained from impedance plot.

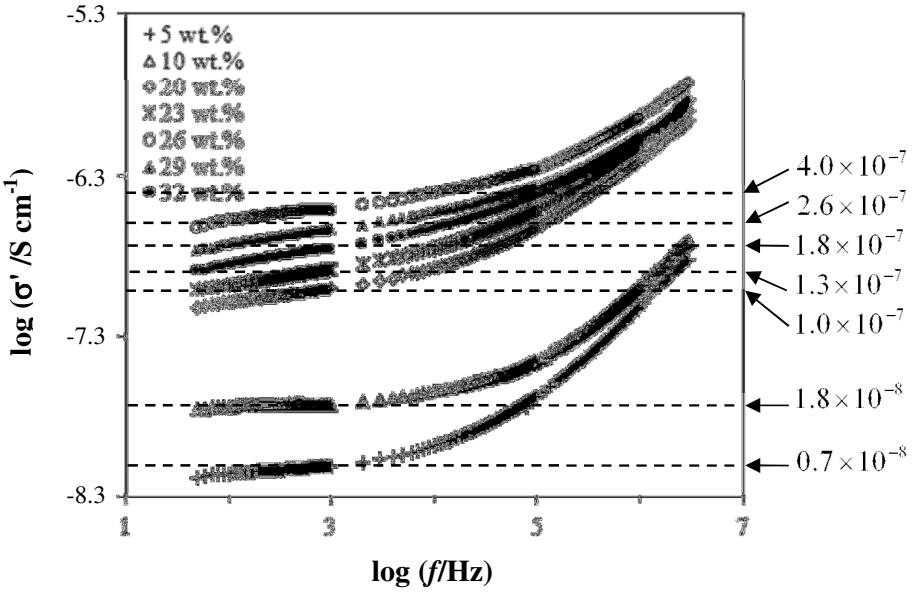

Fig. 7.13. Variation of log σ' versus log *f* for PCL-NH_4SCN films added with 0 to 32 wt.% NH_4SCN at room temperature.

From Fig. 7.13, a nearly frequency independent plateau is observed at low frequency region while a dispersion is depicted at high frequency region. The extrapolation of plateau to zero frequency will give the value of σ_{dc}. For samples without a clear well define plateau, a demarcation frequency is required to show the onset of dc conductivity. This demarcation frequency could be determined by refering to the rapid decrease after the loss tangent peak [Gerhardt, 1994] in Fig. 7.11. The demarcation frequency with the corresponding salt content is depicted in Table 7.1.

Table 7.1
The demarcation frequency for PCL-NH_4SCN films added with 0 to 32 wt.% NH_4SCN, taken from the loss tangent peak.

salt content, (wt.%)	log (*f*/Hz)	*f* (Hz)
5	2.4	250
10	2.8	630
20	2.9	790
23	3.0	1000
26	4.1	12600
29	3.6	3980
32	3.3	2000

The estimated σ_{dc} is shown in Fig. 7.13. It is found to be matching very well with the experimental σ_{dc} as depicted in Fig. 7.3.

7.2.3 Temperature Dependence of Conductivity

The conductivities for complexes of PCL with 10 wt.%, 20 wt.%, 26 wt.% and 32 wt.% are also measured as a function of temperature, from 25 °C to 55 °C in steps of

5 °C. The temperature range is limited by the low melting point of the samples where solid to liquid phase transition would occur. The impedance plots of PCL incorporated with 10 wt.% of NH_4SCN at various temperature in °C are depicted in Fig. 7.14.

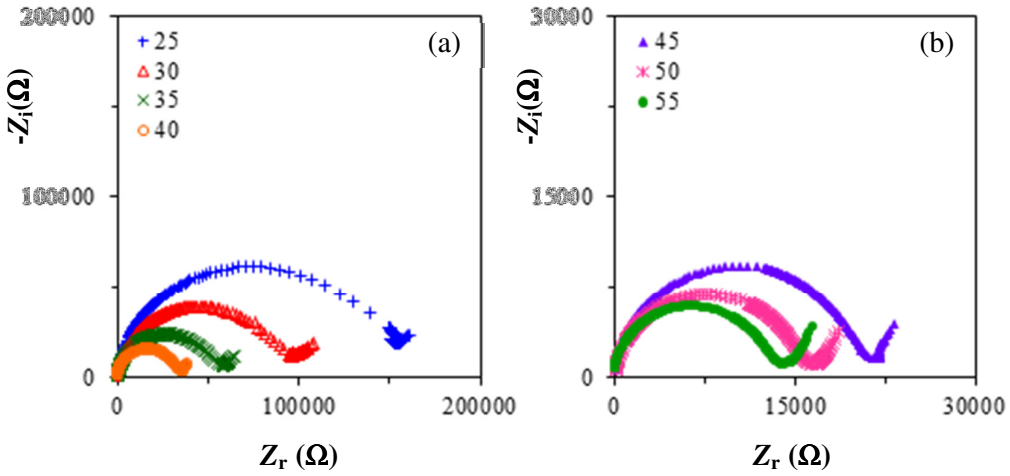

Fig. 7.14. Impedance plot for PCL-NH_4SCN films added with 10 wt.% NH_4SCN at temperature from 25 to 55 °C.

At 25 °C (298.15 K), the impedance plot shows the form of a depressed semicircle. As the temperature rises, the diameter of the depressed semicircles becomes smaller. At the same time, the inclined spike becomes more apparent at the low frequency region. It can be seen clearly that the value of R_b is strongly affected by the temperature and is found to decrease with increasing temperature. This means that dc conductivity is thermally activated and enhances with increasing temperature.

The plot of log σ versus 1000/T for PCL-NH_4SCN polymer electrolyte system is shown in Fig. 7.15.

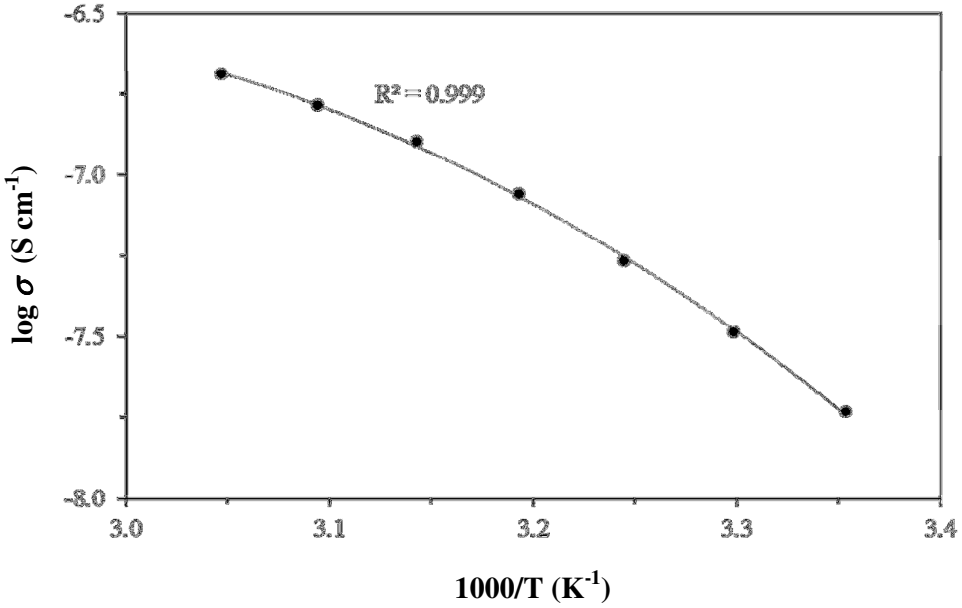

Fig. 7.15. The temperature dependence of conductivity for PCL-NH_4SCN films added with 10 wt.% NH_4SCN.

The regression value, r^2 of the plot is found using both the linear and polynomial trendlines. It is noticed that the polynomial trendline gives r^2 value of 0.999, almost unity. This means the plot fall almost perfectly on a curved line and clearly indicates the temperature dependence conductivity does not follow Arrhenius rule. The relationship of conductivity-temperature is not linear, instead it can be expressed following the Vogel-Tamman-Fulcher (VTF) rule.

According to Geiculescu *et al.*, (2002), the curvature in Fig. 7.15 indicates the mechanical coupling between segmental motion of polymer matrix and ionic motion. This result is in good agreement with the result from electric modulus. A signal peak from M'' versus log f (Fig. 7.9) plot and a depressed semicircle from M'' versus M' plot (Fig. 7.10) predict the coupling between conductivity relaxation and dipolar relaxation.

The impedance plots and temperature dependence of conductivity plots of other PCL samples incorporated with 20, 26 and 32 wt.% of NH_4SCN are displayed in Fig. 7.16 to 7.21, respectively.

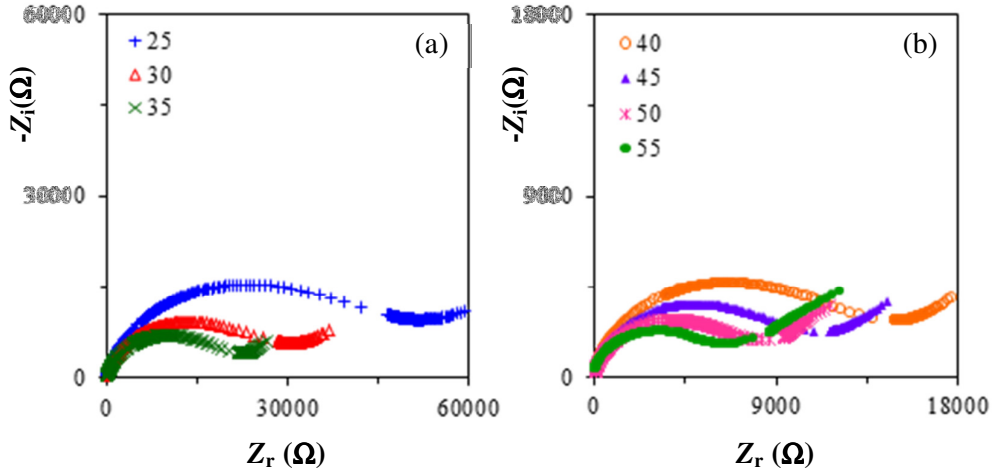

Fig. 7.16. Impedance plot for PCL-NH_4SCN films added with 20 wt.% NH_4SCN at temperature from 25 to 55 °C.

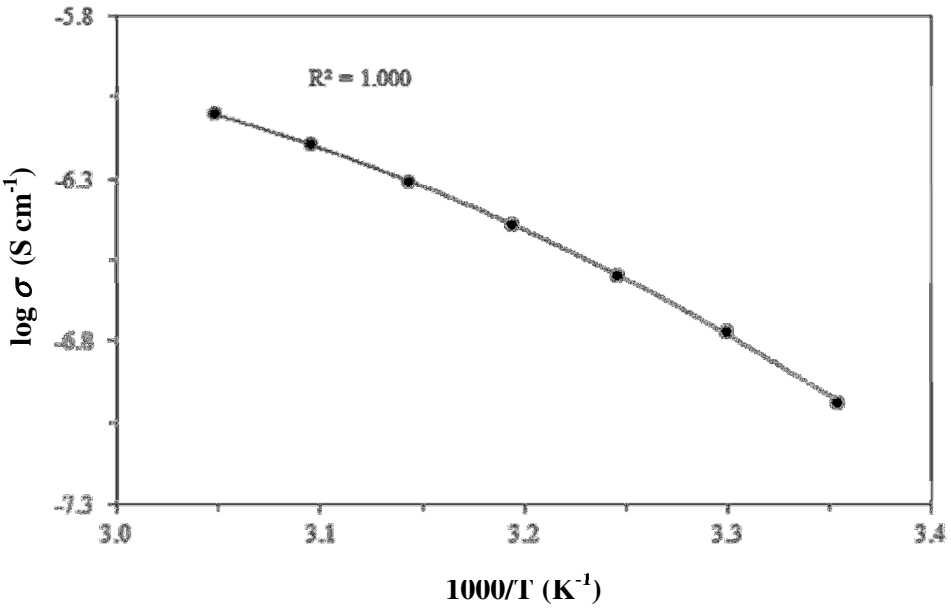

Fig. 7.17. The temperature dependence of conductivity for PCL-NH_4SCN films added with 20 wt.% NH_4SCN.

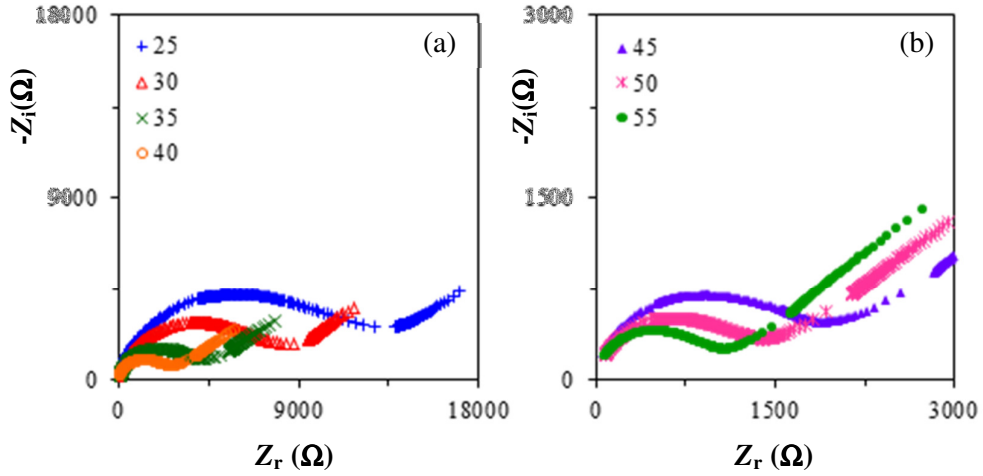

Fig. 7.18. Impedance plot for PCL-NH_4SCN films added with 26 wt.% NH_4SCN at temperature from 25 to 55 °C.

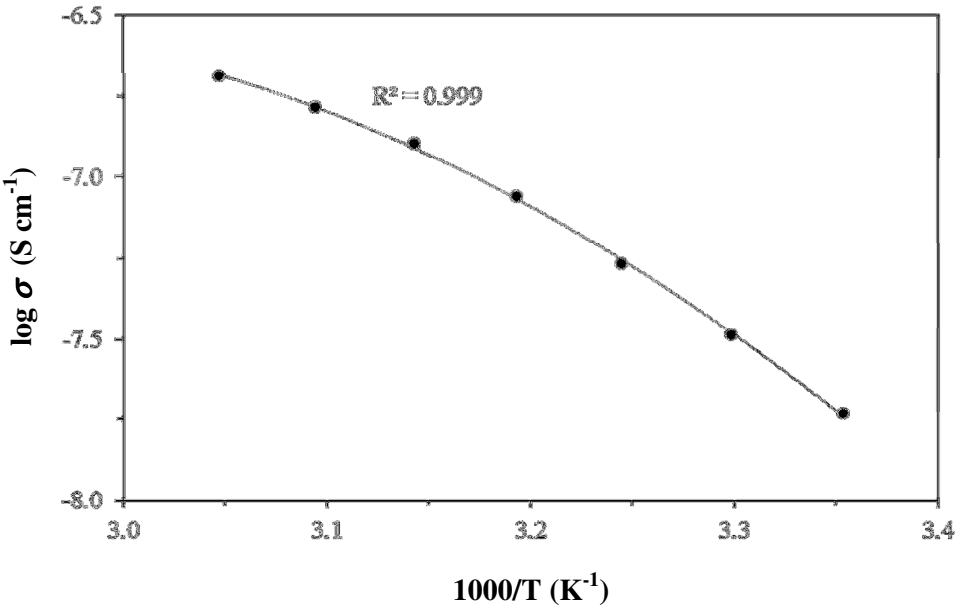

Fig. 7.19. The temperature dependence of conductivity for PCL-NH_4SCN films added with 26 wt.% NH_4SCN.

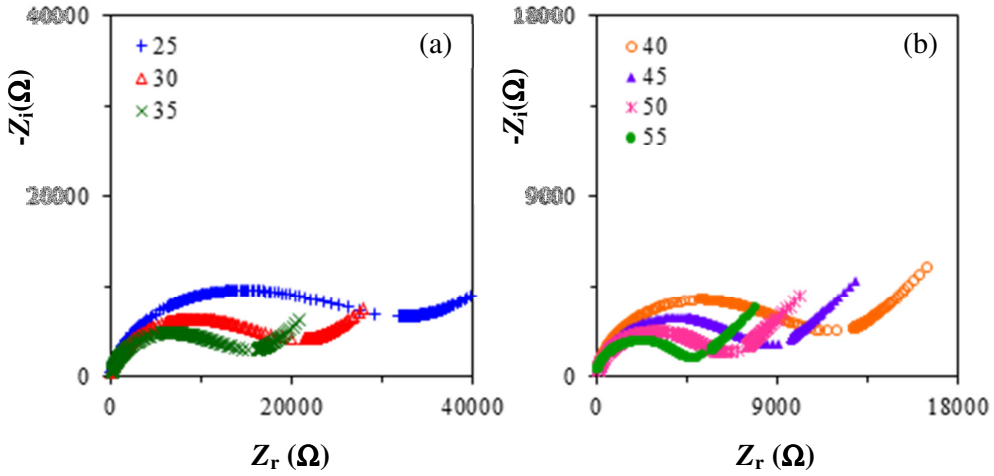

Fig. 7.20. Impedance plot for PCL-NH4SCN films added with 32 wt.% NH4SCN at temperature from 25 to 55 °C.

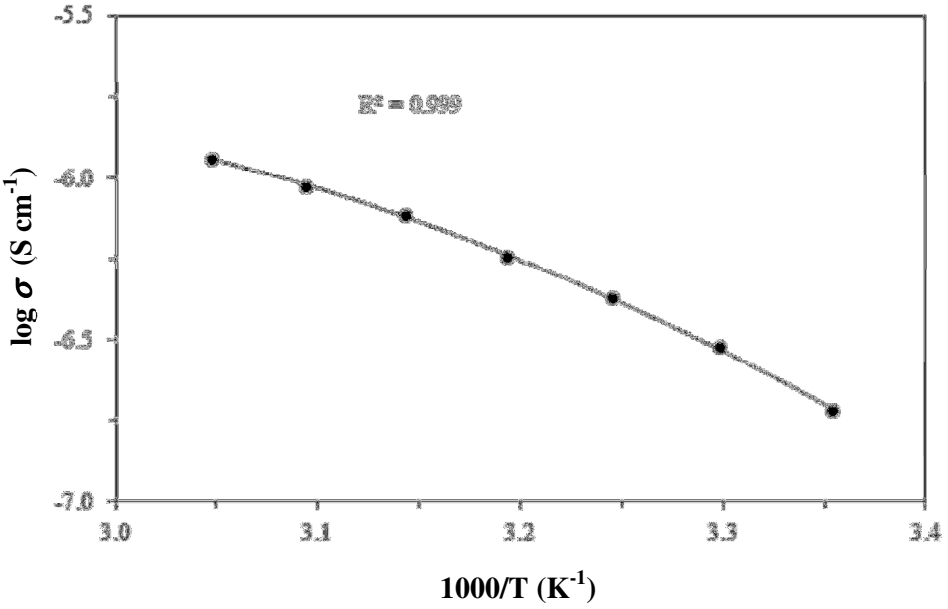

Fig. 7.21. The temperature dependence of conductivity for PCL-NH_4SCN films added with 32 wt.% NH_4SCN.

All results for samples added with 20, 26 and 32 wt.% NH_4SCN demonstrate similar features, a depressed semicircle at the high frequency region followed by an inclined spike at the low frequency region. The value of R_b for all samples decreases

with increasing temperature, indicating that dc conductivity enhances with increasing temperature.

The polynomial trendline gives r^2 close to unity for all the log σ versus 1000/T plots. This also reveals that the temperature dependence conductivity follow the Vogel-Tamman-Fulcher (VTF) rule. The VTF equation can be expressed as [MacCallum and Vincent, 1987]:

$$\ln \sigma T^{0.5} = \ln A - \frac{B}{(T - T_0)} \tag{7.4}$$

Here A is the pre-exponential factor in units of $S\ m^{-1}\ K^{0.5}$ which is reflecting the number density of charge carriers, B is the pseudo energy in unit of K that represents the energy required to create adequate free volume for polymer segment mobility, T is absolute temperature and T_0 is the quasi-equilibrium glass transition temperature at which free volume disappears or ionic conduction becomes frozen. T_0 is usually 50 K lower than T_g [Qian *et al.*, 2002].

Temperature dependence of conductivity at various NH_4SCN content is plotted in Fig. 7.22 using VTF equation for the linear fit. Table 7.1 displays the VTF parameters determined by fitting the experimental data. T_0 was obtained by trial and error beginning from $(T_g - 50)$ and was subsequently changed to get the maximum regression value approaching unity. T_g values are obtained from DSC results, in Section 4.2 (Table 4.1).

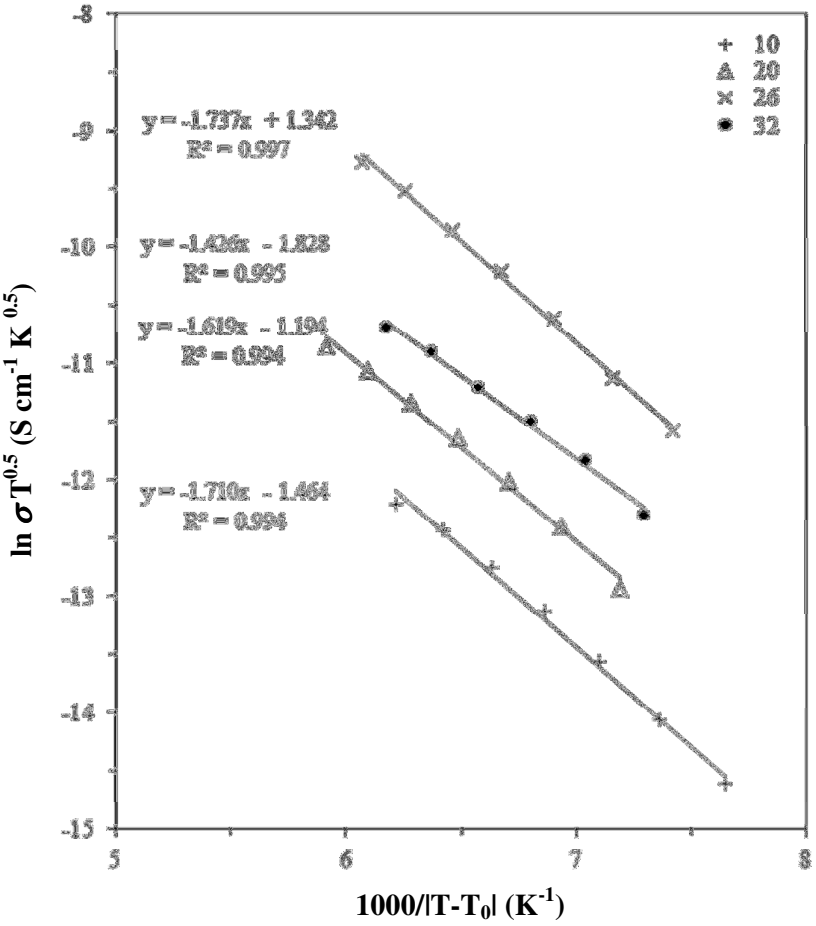

Fig. 7.22. The VTF temperature dependence of conductivity for PCL-NH_4SCN films added with 0 to 32 wt.% NH_4SCN.

Table 7.1
The VTF fitted parameters from temperature dependence of conductivity for PCL-NH_4SCN films added with 0 to 32 wt.% NH_4SCN.

salt content, (wt.%)	T_g (K)	R^2	VTF fit			$(T_g - T_0)$ (K)
			T_0 (K)	A (S m^{-1} $K^{0.5}$)	B (x 10^3 K)	
10	208.45	0.994	167.35	23.1	1.71	41.1
20	208.55	0.994	159.05	30.3	1.62	49.5
26	208.85	0.997	163.35	382.7	1.74	45.5
32	209.25	0.995	161.15	16.1	1.43	48.1

Fig. 7.22 shows a reasonably good fit of conductivity to the VTF equation with regression value of ~0.994-0.997 for selected samples. These demonstrate the close coupling between the ionic motion and the polymer segmental motion [Karan *et al*., 2008]. This result is in agreement with Section 7.2.2 (Fig. 7.10) that predicts the coupling motions which exhibit both conductivity and dipolar relaxations.

The pre-exponential factor *A* is found to increase with increasing NH_4SCN concentration up to 26 wt.%. The increasing trend of parameter *A* was reported in other polymer electrolyte systems such as PEO-$LiCF_3SO_3$ [Karan *et al*., 2008] and poly(ethylene oxide-co-propylene oxide) (P(EO/PO))-LiTFSI [Seki *et al*., 2005]. The parameter *B* is unexpectedly observed to fluctuate with NH_4SCN content, it reduces initially and rises again at 26 wt.% NH_4SCN. Such observation was also reported in PEO-based systems [Karan *et al*., 2008]. Cruickshank *et al*. (1995) reported an increasing trend of parameter *B* in PEG-based system added with various salts such as $LiCF_3SO_3$, $LiClO_4$, $NaClO_4$, $LiBF_4$ and $NaBF_4$. The value of parameter *B* is calculated to be in the range of 10^3 K (10^{-1} eV or 10 kJ mol^{-1}). This is of the same magnitude as reported for other polymer-salt systems [Cruickshank *et al*., 1995; Seki *et al*., 2005; Karan *et al*., 2008].

7.2.4 Temperature Dependence of Dielectric Behavior

A sample at 32 wt.% NH_4SCN is used for temperature dependent dielectric study. Plots of log ε' and ε'' as a function of log *f* at temperatures from 25 to 55 °C are illustrated in Fig. 7.23 and 7.24, respectively.

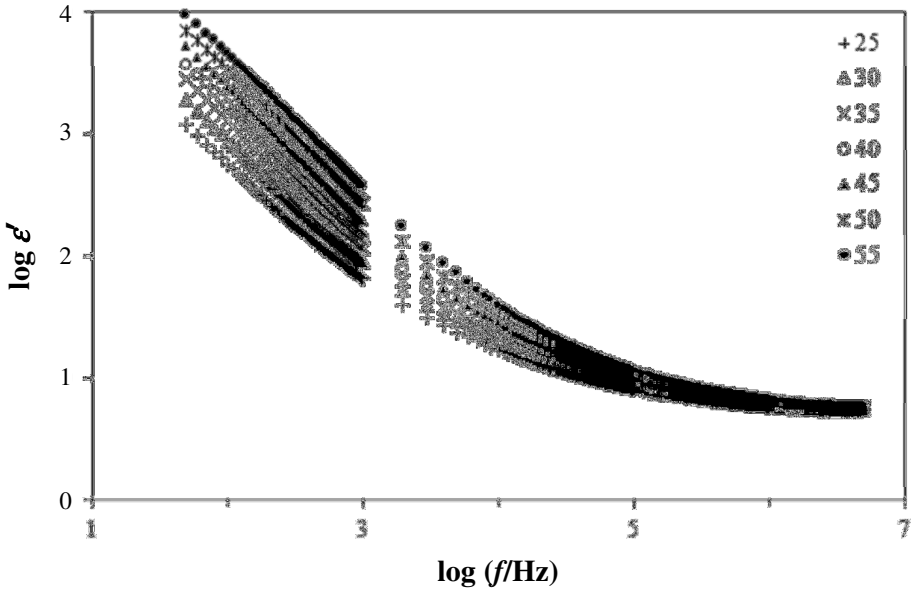

Fig. 7.23. Variation of log ε' versus log f for PCL-NH_4SCN films added with 32 wt.% NH_4SCN at temperature from 25 to 55 °C.

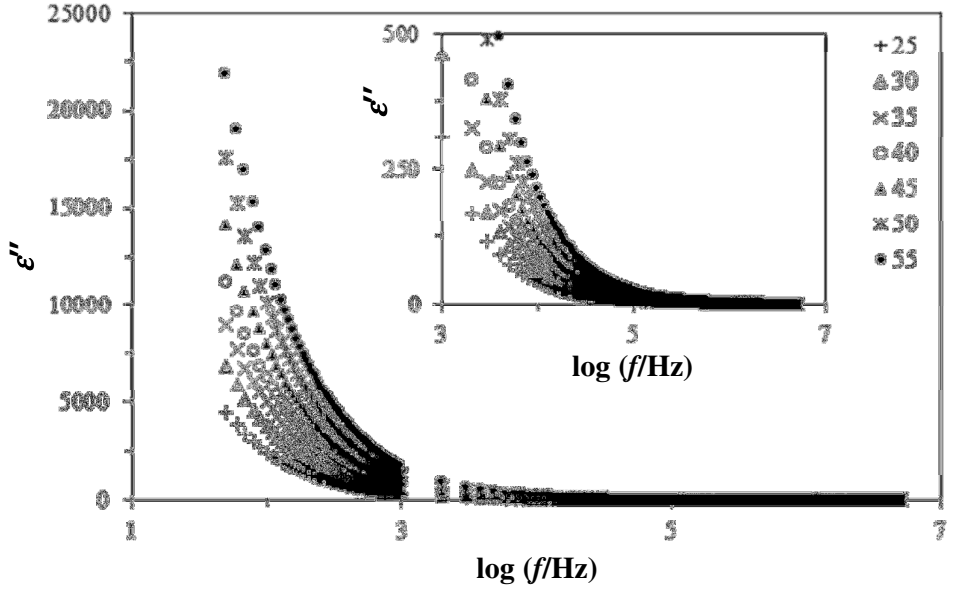

Fig. 7.24. Variation of ε'' versus log f for PCL-NH_4SCN films added with 32 wt.% NH_4SCN at temperature from 25 to 55 °C. Inset displays the magnified graph.

In the low frequency region, both ε' and ε'' show dispersion due to electrode polarization effect. As described in Section 7.2.2, ε' is an indicator of the amount of dipoles in the PE system. It is clear that ε' increases with elevating temperature. The motion of dipoles is facilitated with the increase of temperature and thereby ε' is increased [Sheba and Mansy, 2008].

The electric modulus plots for the same system at different temperatures are depicted in Fig. 7.25 and 7.26.

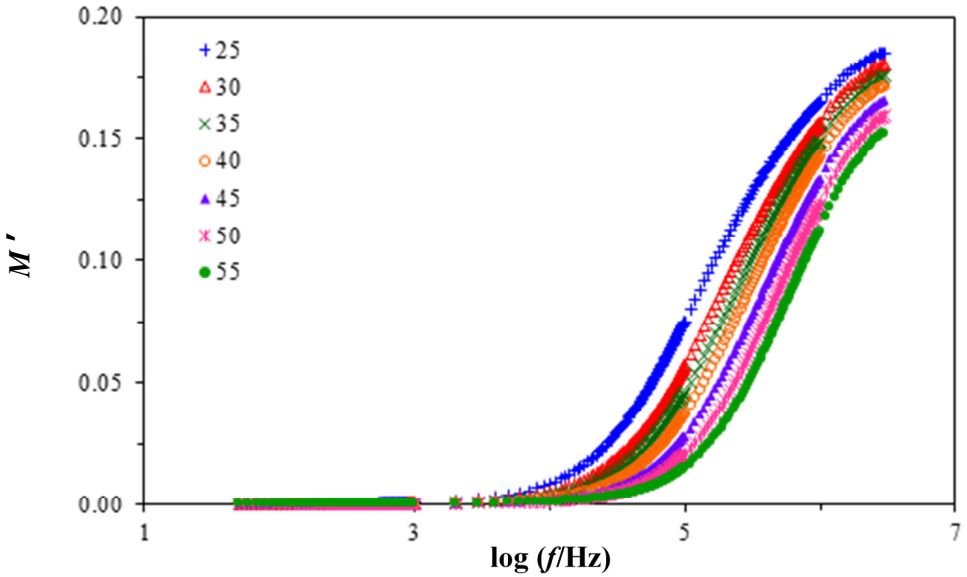

Fig. 7.25. Variation of M' versus $\log f$ for PCL-NH_4SCN films added with 32 wt.% NH_4SCN at temperature from 25 to 55 °C.

M' versus frequency plot shows the sigmoidal curve that decreases in value with increasing temperature, as expected in the reciprocal relationship with ε'. On the other hand, M'' curve gives a single and asymmetric peak that is attributed to the coupling of conductivity relaxation and dipolar relaxation. As temperature elevates, the dispersion peak of M'' is seen to shift towards higher frequency.

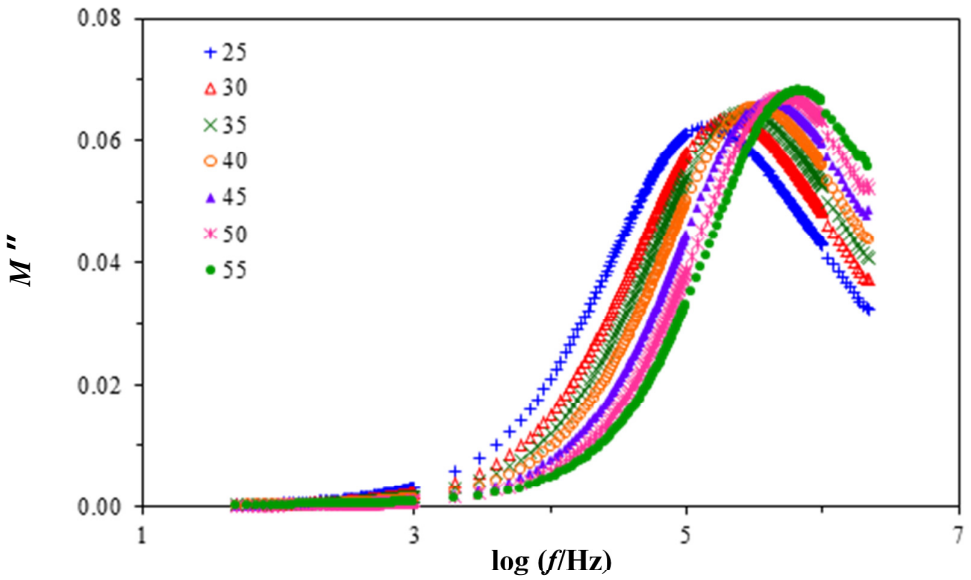

Fig. 7.26. Variation of M'' versus log *f* for PCL-NH_4SCN films added with 32 wt.% NH_4SCN at temperature from 25 to 55 °C.

Fig. 7.27 depicts the variation of loss tangent as a function of frequency at temperatures from 25 to 55 °C.

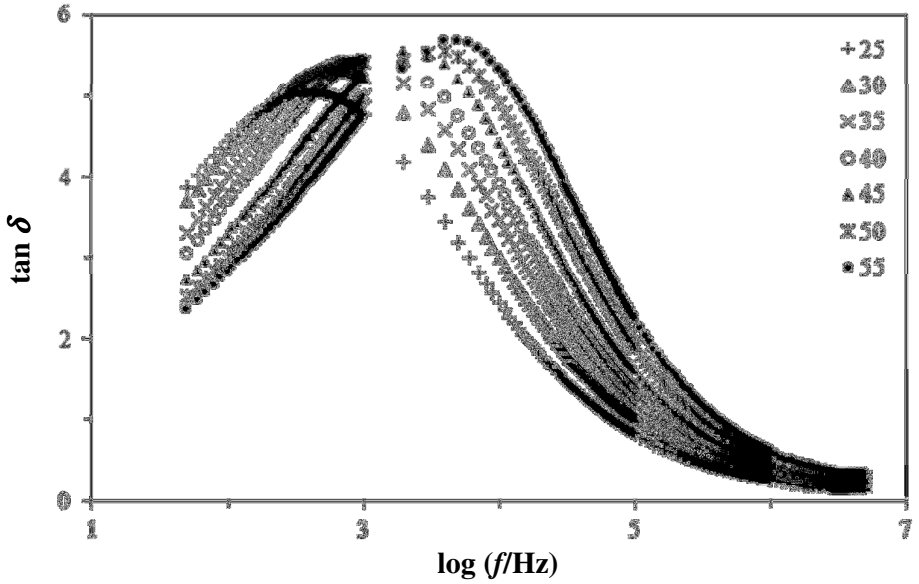

Fig.7.27. Variation of loss tangent versus log *f* for PCL-NH_4SCN films added with 32 wt.% NH_4SCN at temperature from 25 to 55 °C.

Single and non-symmetric well defined peak is observed in Fig. 7.27 for each temperature. As temperature rises, the loss tangent peak shifts to the right indicating a reducing relaxation time. Corresponding to that, the loss tangent peak height increases as well, which can be attributed to the drop of resistivity of the system [Prabakar *et al*., 2003]. This means more ions are available for the ionic conduction. The effect of temperature from Fig. 7.25 to 7.27 can be summarized as follows. When temperature increases, the crystalline phase of PCL dissolves progressively into amorphous phase. PCL matrix becomes more flexible with minimum internal friction. The orientation of PCL dipoles and motion of salt ions are faster. These lead to an increase of ε' value [Saroj and Singh, 2012] and subsequently reduce the relaxation time [Karmakar and Ghosh, 2012] of the coupling between polymer segmental motion and ionic motion.

The temperature dependence of the real part of complex conductivity versus log *f* for the same 32 wt.% salt content are displayed in Fig.7.28.

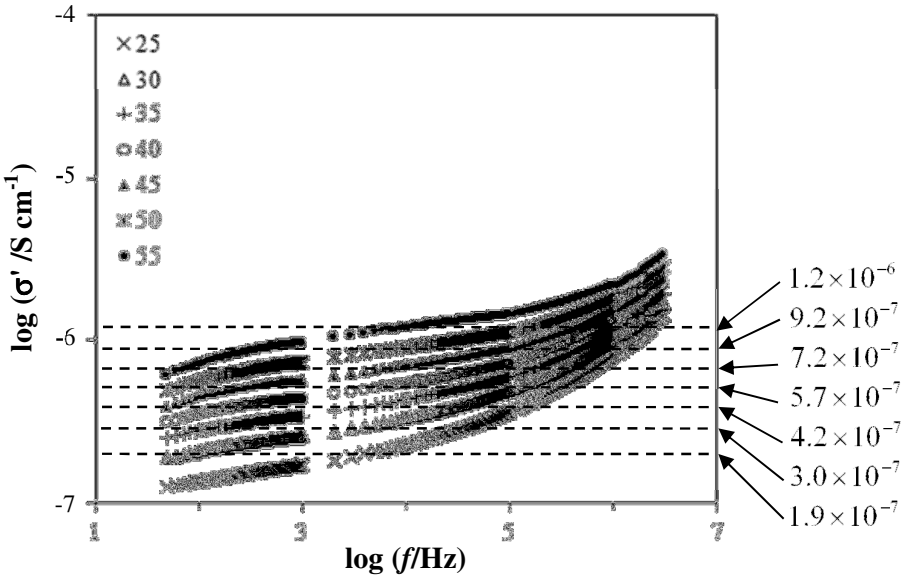

Fig. 7.28. Variation of log σ' versus log *f* for PCL-NH_4SCN films added with 32 wt.% NH_4SCN at temperature from 25 to 55 °C.

At all temperatures, the graph shows a plateau at low frequency region and dispersion at higher frequency. The plateau can be extrapolated to zero frequency estimating the value of σ_{dc}. As temperature rises, the plateau moves up consistently. This shows that σ_{dc} is thermally assisted and the estimated σ_{dc} matches very well with the experimental σ_{dc}.

7.3 Electrical Studies of PCL-NH_4SCN-EC system

The highest room temperature conductivity for PCL-NH_4SCN system is 3.94 x 10^{-7} S cm^{-1}, achieved at 26 wt.% NH_4SCN. This value is considerably low for practical applications. In order to overcome this drawback, efforts have been made to enhance the conductivity of the system through plasticization. Therefore, EC is added to the most conducting PCL-NH_4SCN sample. The objective of the current study is to investigate the effect of EC on the electrical properties of PCL-NH_4SCN samples.

7.3.1 Composition Dependence of Conductivity

The impedance plots of PCL-NH_4SCN-EC films with 0 to 50 wt.% EC at room temperature are presented in Fig. 7.29.

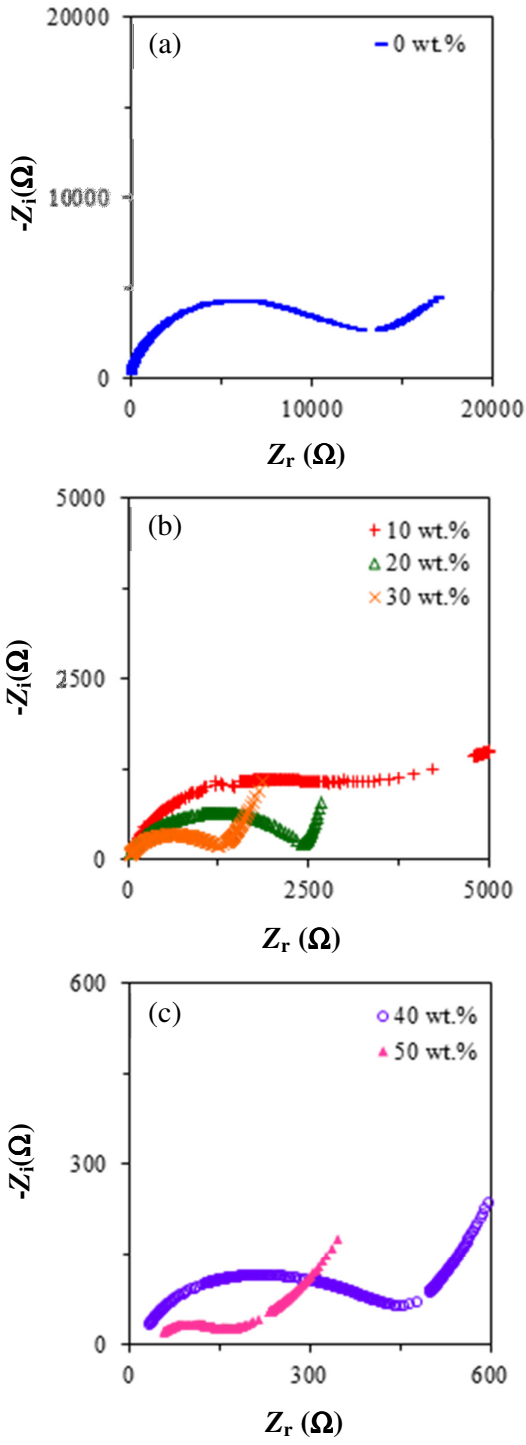

Fig. 7.29. Impedance plot for PCL-NH_4SCN-EC films added with 0 to 50 wt.% EC at room temperature.

Generally, the impedance plots show a depressed semicircle at high frequency region followed by an inclined spike at low frequency region. For samples containing 10, 20 and 30 wt.% EC in Fig. 7.29 (b), the R_b value are obtained at 3900 Ω, 2400 Ω and 1320 Ω, respectively. As the EC content increases, the diameter of the depressed semicircle reduces and the spike becomes longer. The R_b value for 40 and 50 wt.% as illustrated in Fig. 7.29 (c) are obtained to be 505 and 170 Ω, respectively. These R_b values are then used to calculate the conductivity of the corresponding samples.

The experimental data is also fitted by an equivalent circuit as discussed in Section 7.2.1. Fig. 7.30 presents the fitting of the equivalent circuit to the experimental data of PCL-NH_4SCN-EC films added with 30 wt.% EC. The solid line and circle marker represent the fitted data and the experimental data, respectively.

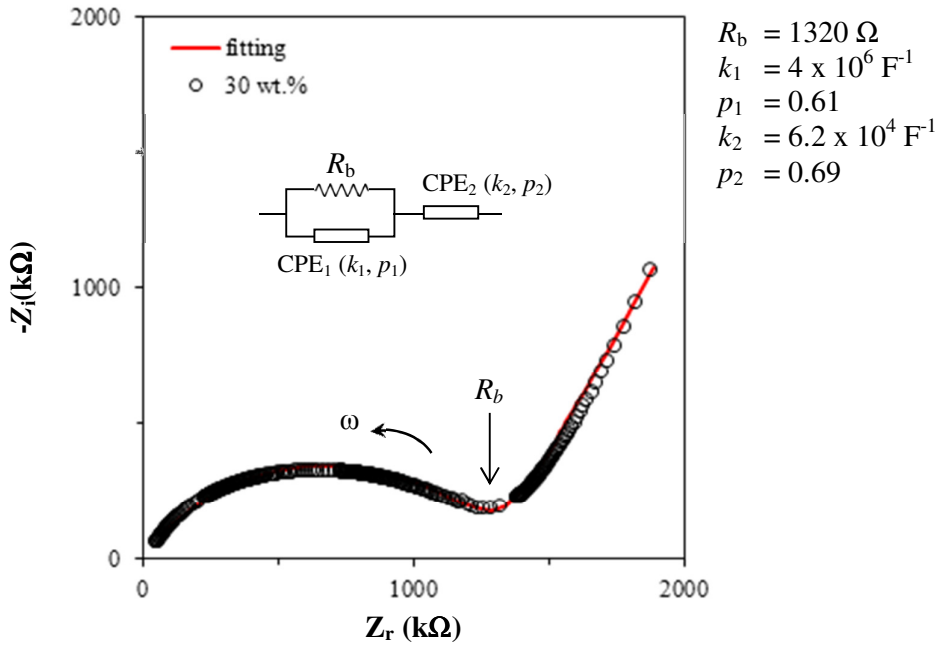

Fig. 7.30. Fitting of the equivalent circuit to the experimental data of PCL-NH_4SCN-EC films added with 30 wt.% EC.

It can be depicted that the fitted data overlay on top of the experimental data showing a good match of the fitting. Parameters such as k_1, p_1, R_b, k_2 and p_2 are obtained to be 4×10^6 F^{-1}, 0.61, 1320 Ω, 6.2×10^4 F^{-1} and 0.69, respectively.

The variation of room temperature conductivity as a function of EC concentration is depicted in Fig. 7.31.

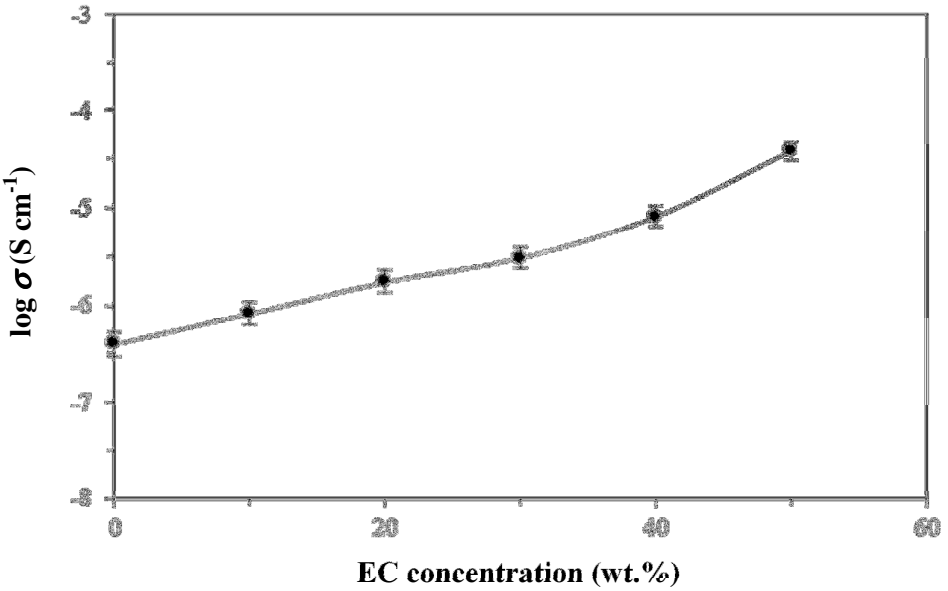

Fig. 7.31. EC concentration dependence of dc conductivity for PCL-NH_4SCN-EC films at room temperature.

Upon addition of 10 wt.% EC, the room temperature conductivity increases from 3.9×10^{-7} S cm^{-1} of the highest conducting polymer-salt complex to 8.2×10^{-7} S cm^{-1}. Conductivity continues to increase monotonically with increasing EC content up to 3.8×10^{-5} S cm^{-1} at 50 wt.% EC. This indicates that the polymer is capable of accomodating a large amount of EC molecules. The increase of conductivity with increasing EC content is attributed to the enhancement of ion density and ion mobility which will be explained in the following section.

7.3.2 Composition Dependence of Dielectric Behavior

Fig. 7.32 shows the plot of ε' versus log f for PCL-NH_4SCN-EC films added with 0 to 50 wt.% EC at room temperature**.**

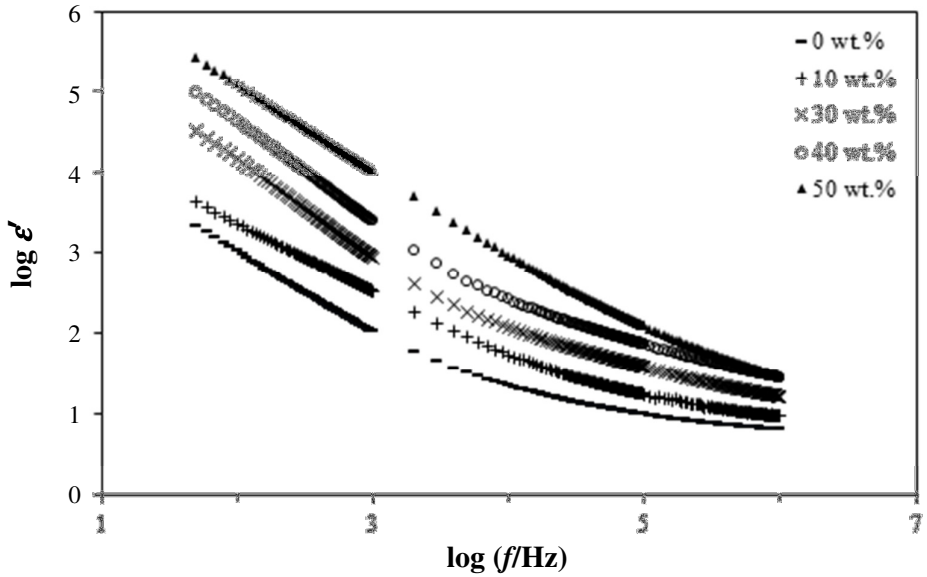

Fig. 7.32. Variation of log ε' versus log f for PCL-NH_4SCN-EC films added with 0 to 50 wt.% EC at room temperature.

The value of ε' builds up exponentially with decreasing frequencies and is attributed to electrode polarization, a result of space charge accumulation. At high frequency region, ε' drops drastically and eventually saturate because the ions can no longer follow the fast reversing electric field.

The variation of ε' with EC content is observed to follow the same trend as in the in conductivity-EC composition relationship. Refer to Fig. 7.32, the addition of EC into polymer-salt complexes seem to amplify the value of ε' many folds. The ε' value of the unplasticized film is only around 10^3 at low frequency as shown in Fig. 7.4.

Addition of 30 wt.% and 50 wt.% EC have moved ε' value up 10 times and 100 times, respectively. The ε' value at 50 wt.% EC plasticization is as high as 2.7×10^5.

A plot of EC concentration dependence of real relative permittivity for PCL-NH_4SCN-EC films at selected frequencies is depicted in Fig. 7.33 to shed some light on the conductivity study.

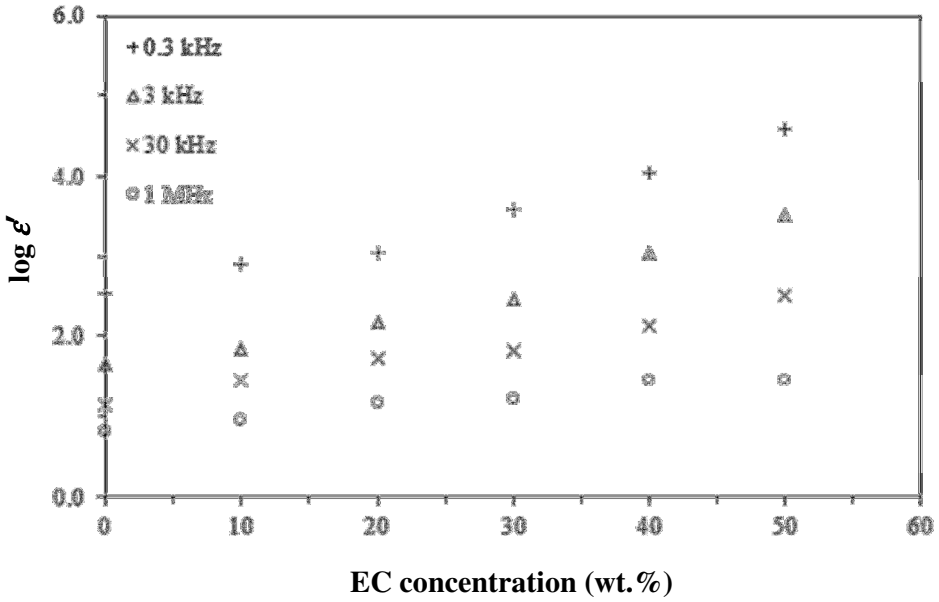

Fig. 7.33. EC concentration dependence of log ε' for PCL-NH_4SCN-EC films at selected frequencies.

For all the selected frequencies in Fig. 7.33, it is observed that ε' increases with increasing EC content. On comparison to Fig. 7.31, it is the same trend as the conductivity plot. In other words, the increase of electrolyte relative permittivity does play an important role in conductivity enhancement. For PCL-NH_4SCN system in Section 7.2.2, it can be deduced that ε' reflects the number density of free ions. Higher ε' means more free ions thus leading to higher conductivity.

For PCL-NH_4SCN-EC system, it is good to plot conductivity versus ε' in order to paint a better picture of the correlation between σ and ε'. Fig. 7.34 presents the conductivity as a function of ε' at selected frequencies.

A strong dependence of conductivity on ε' value is revealed in Fig.7.34. It is good to recall that similar observation is obtained for PCL-NH_4SCN system in Fig. 7.6. In the current PCL-NH_4SCN-EC system, the ε' value is determined by the injecting EC content. This result seems to agree with the proposal that the dependence of the dc conductivity on the system relative permittivity is contained in the exponential prefactor term of the Arrhenius equation [Petrowsky and Frech, 2008; 2009].

Fig. 7.35 show the plot of ε'' versus log *f* for PCL-NH_4SCN-EC films added with 0 to 50 wt.% EC at room temperature**.** The dispersion at low frequencies is attributed to the energy losses caused by electrode polarization. As frequency increases, energy losses due to the charge carriers decrease until saturation. It can also be seen that addition of EC resulted in a higher number density of charges in which they generate more heat loss. No appreciable relaxation peak is depicted in the studied frequency range. From Section 7.2.2, this is expected because the large amount of electrode polarization could mask the small dipolar relaxation peak.

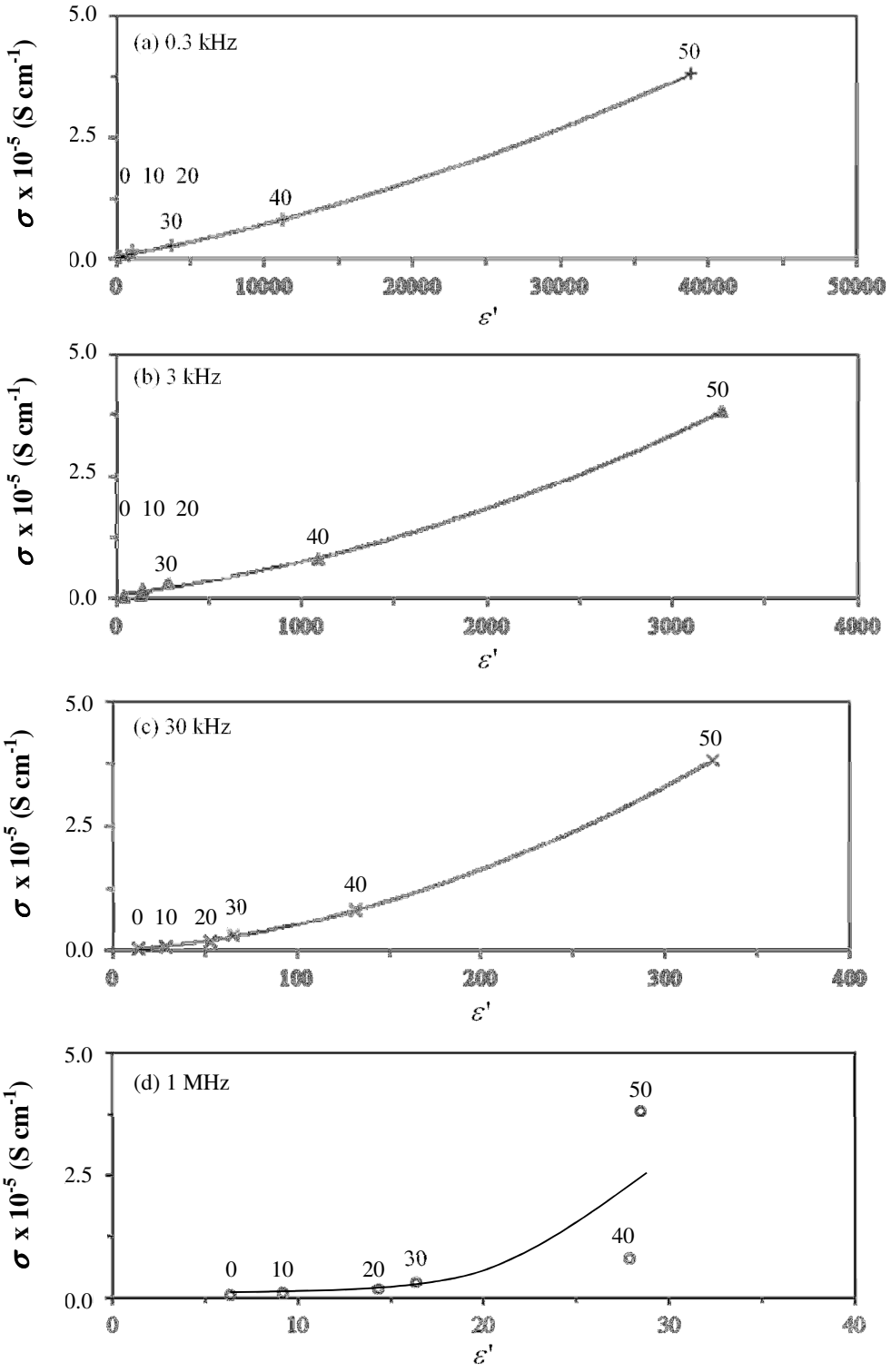

Fig. 7.34. Conductivity as a function of ε' at selected frequencies. EC concentrations in wt.% are labeled within the figures. The line is just a guide to the eye.

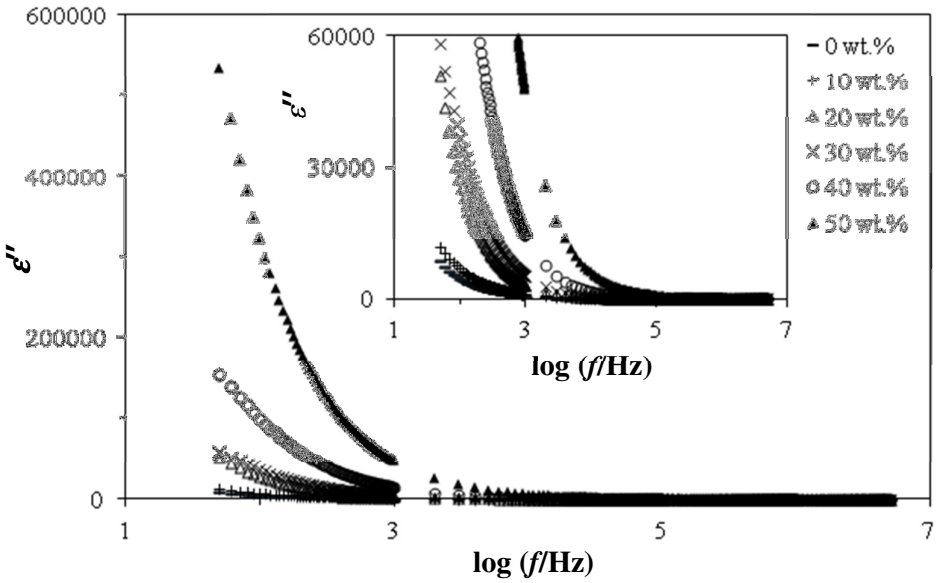

Fig. 7.35. Variation of ε'' versus log f for PCL-NH_4SCN-EC films added with 0 to 50 wt.% EC at room temperature. Inset displays the magnified graph.

The M' and M'' as a function of frequency for PCL-NH_4SCN-EC films added with 0 to 50 wt.% EC at room temperature are shown in Fig. 7.36. and 7.37.

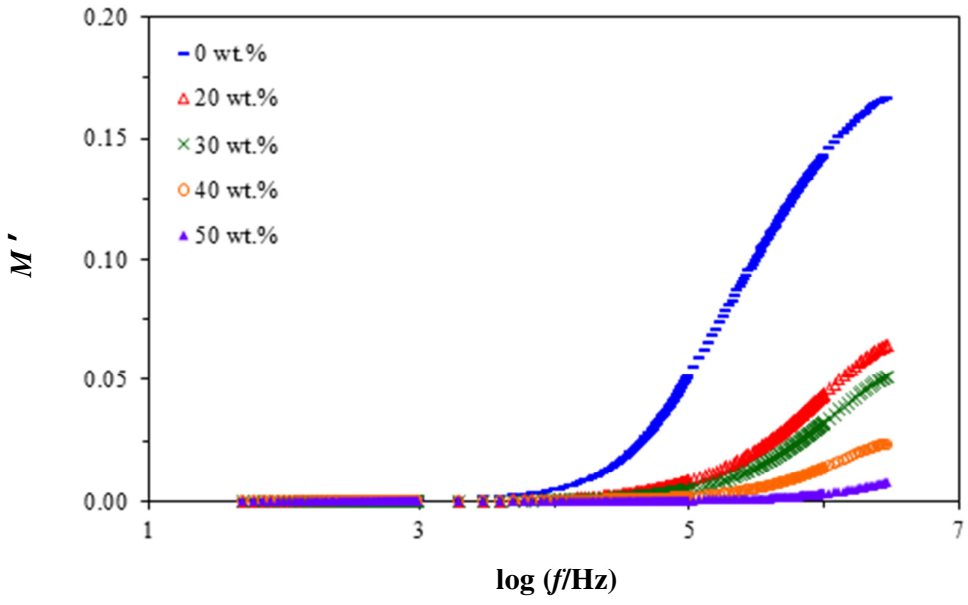

Fig. 7.36. Variation of M' versus log f for PCL-NH_4SCN-EC films added with 0 to 50 wt.% EC at room temperature.

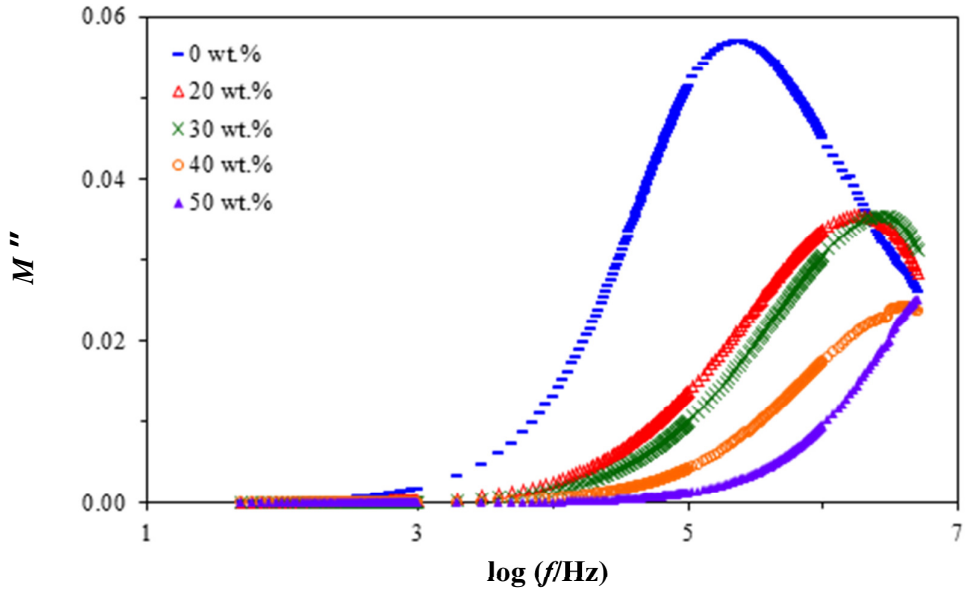

Fig. 7.37. Variation of M'' versus log f for PCL-NH_4SCN-EC films added with 0 to 50 wt.% EC at room temperature.

Fig. 7.36 shows a similar long tail as in Fig. 7.8 at low frequency region which is attributed to the large capacitance effect. The sigmoidal shape of M' at high frequency region shifts to the right and reduces in value as more salt is incorporated. In M'' versus log f plot, a single and asymmetric peak is depicted at 1.7 and 2.9 MHz for samples added with 20 and 30 wt.% EC, respectively. As EC concentration increases, this broad peak is observed to shift to the right towards higher frequency and the corresponding peak height reduces. This indicate a reducing relaxation time.

The variation of the curves is the same as the variation of conductivity in Fig. 7.31. The FWHM of the M'' peak is also greater than 1.144 decades as obtained in PCL-NH_4SCN system, manifesting a non-Debye distribution of relaxation times. The argand plot of M'' versus M' for PCL- NH_4SCN-EC films added with 0 to 50 wt.% EC is plotted in Fig. 7.38.

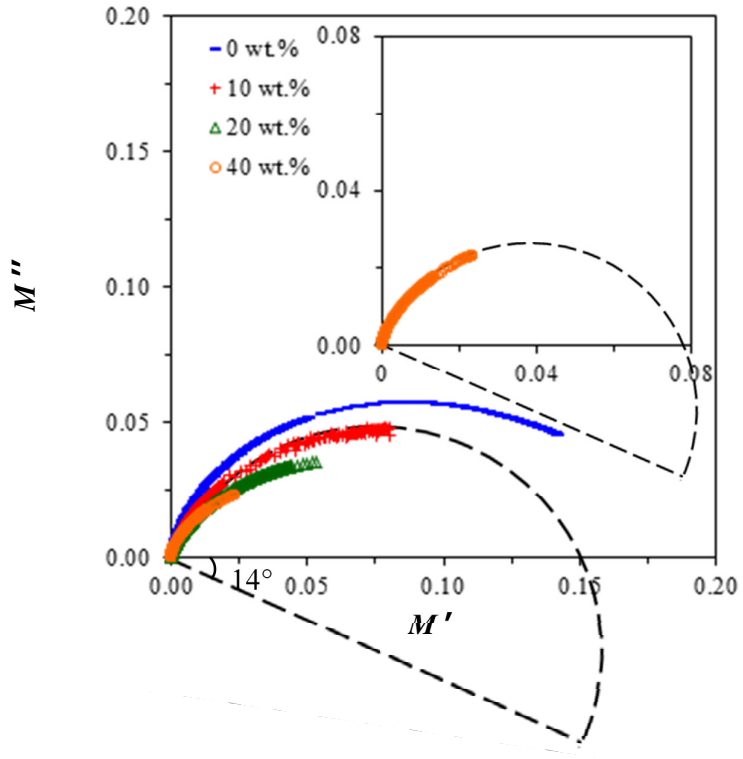

Fig. 7.38. Argand plot of M'' versus M' for PCL-NH_4SCN-EC films added with 0 to 50 wt.% EC. Inset shows the magnified graph for 40 wt.% EC.

A depressed semicircle arc passing through the origin is shown in Fig. 7.38. Similar observation is found as in PCL-NH_4SCN system but the present system shows a greater tilt angle of 14° to the horizontal axis. The translational diffusion of ions is most probably coupled with the orientational dipolar relaxation mode at room temperature (25 °C), which is much higher than the glass transisiton temperature, T_g (below -60 °C). Thus, the M'' peak frequency indicates the transition from long range conductivity relaxation to short range dipolar relaxation at increasing frequency [Padmasree *et al*., 2006].

The variation of loss tangent as a function of frequency for PCL-NH_4SCN-EC system is analyzed in Fig. 7.39. The relevant relaxation time was also calculated and shown in Fig. 7.40.

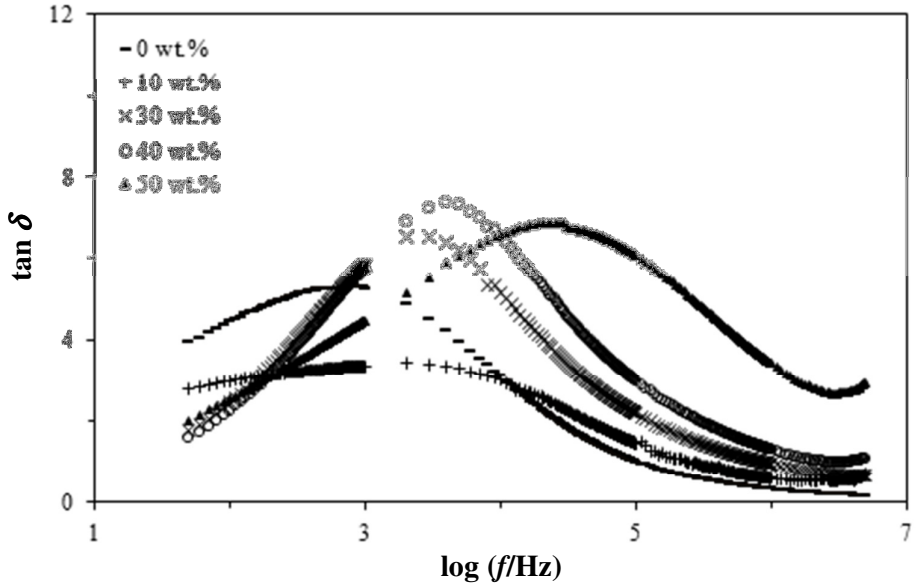

Fig.7.39. Variation of loss tangent versus log *f* for PCL-NH_4SCN-EC films added with 0 to 50 wt.% EC at room temperature.

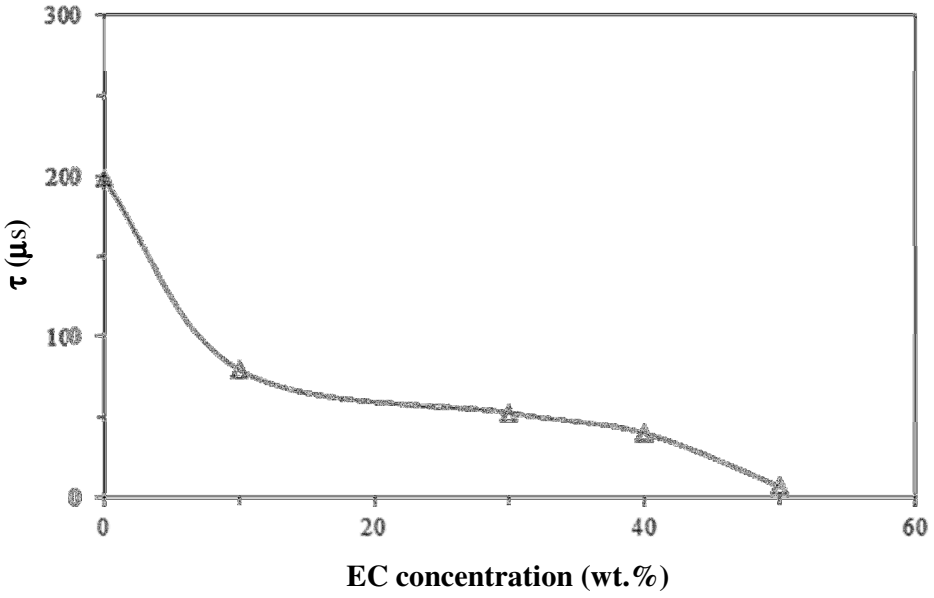

Fig. 7.40. EC concentration dependence of relaxation time at room temperature.

The loss tangent in Fig. 7.39 consists of a well-defined peak at all EC compositions. This non-symmetry peak shifts towards higher frequency as EC content increases, indicating a reduction in the ion relaxation time. Fig. 7.40 depicts the variation of relaxation time which is the inverse of dc conductivity as depicted in Fig. 7.31. The shortest relaxation time is observed at 50 wt.% EC which is the most conducting sample in PCL-NH_4SCN-EC system.

The real part of complex conductivity, is presented in Fig. 7.41.

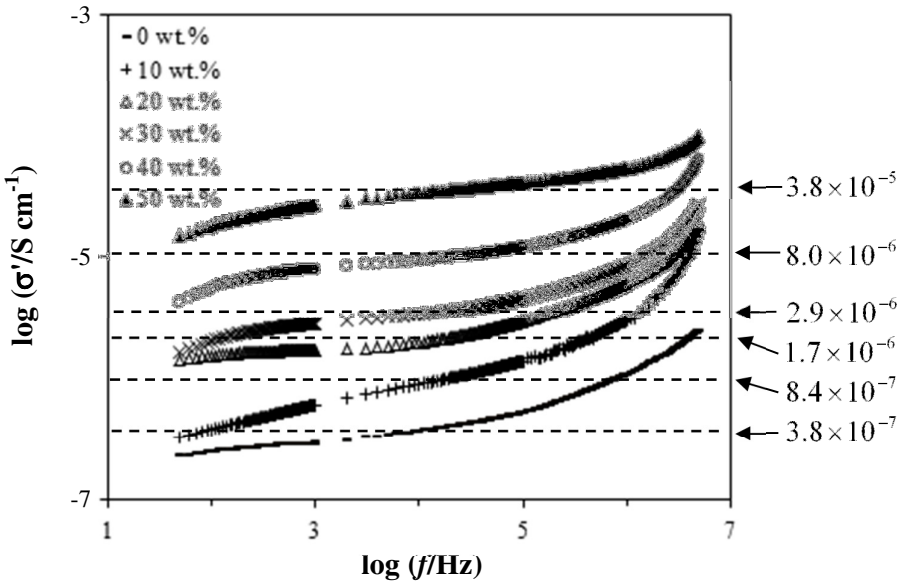

Fig. 7.41. Variation of log σ' versus log *f* for PCL-NH_4SCN-EC films added with 0 to 50 wt.% EC at room temperature.

From Fig. 7.41, a decreasing dispersion is depicted at low fequency region, a nearly frequency independent plateau is observed at middle frequency range while an increaisng dispersion is manifested at the high frequency region. The dispersion at low frequency is attributed to the electrode polarisation effect [Govindaraj and Mariappan,

2002]. By drawing a horizontal line parallel to the plateau and the point it intersects with the vertical axis will give the estimated value of σ_{dc}. The estimated σ_{dc} as shown in Fig. 7.41 match very well with the experimental σ_{dc} as depicted in Fig. 7.31.

7.3.3 Temperature Dependence of Conductivity

The temperature dependent conductivity for PCL-NH_4SCN-EC films were determined at temperatures from 25 to 45 or 50 °C (depending on the melting point) in steps of 5 °C. The impedance plots at various temperatures in °C for PCL-NH_4SCN-EC films incorporated with 20, 30 and 40 wt.% EC are depicted in Fig. 7.42, 7.44 and 7.46, respectively. The corresponding Arrhenius plot of log σ versus 1000/T are shown in Fig. 7.43, 7.45 and 7.47.

From the impedance plots, all PCL-NH_4SCN-EC samples demonstrate similar features, a depressed semicircle at the high frequency region followed by a tilted spike at the low frequency region. As the temperature increases, the diameter of the semicircle becomes smaller indicating a reducing value of R_b. This shows that dc conductivity is thermally activated and enhances with elevating temperature.

From the Arrhenius plots, the regression values of the polynomial trendlines are found to be in the range of 0.993 to unity. This reflects that the plot fall almost perfectly on a curved line. Therefore, the relationship of conductivity-temperature can best be expressed by the Vogel-Tamman-Fulcher rule.

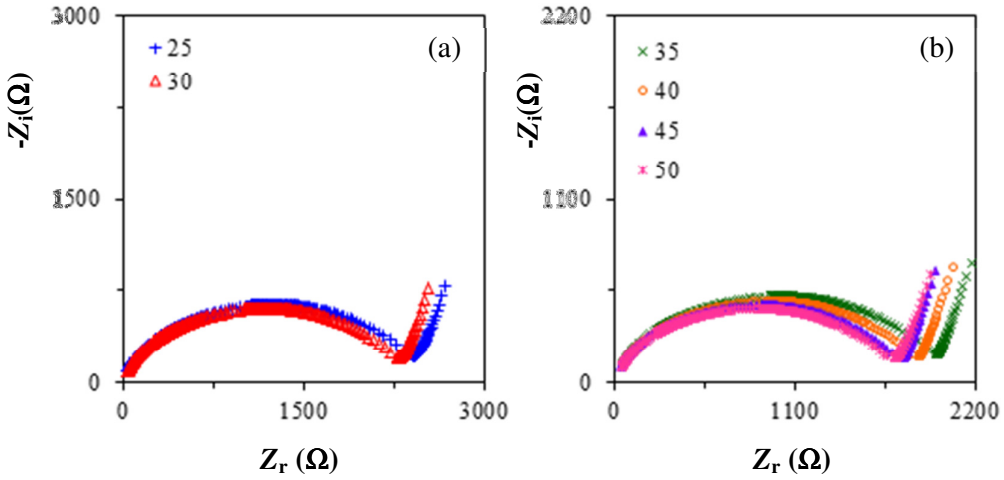

Fig. 7.42. Impedance plot for PCL-NH_4SCN-EC films added with 20 wt.% EC at temperature from 25 to 50 °C.

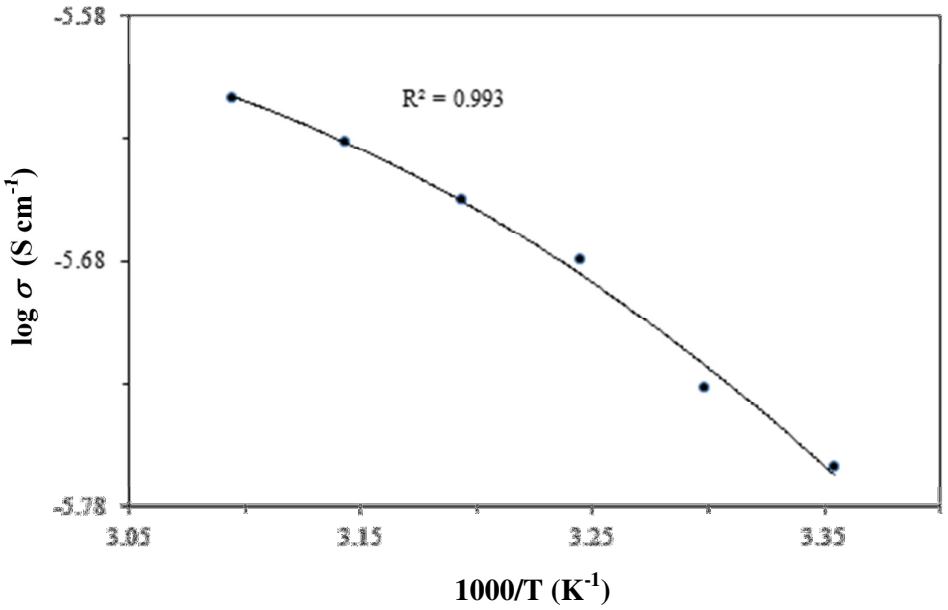

Fig. 7.43. The temperature dependence of conductivity for PCL-NH4SCN-EC films added with 20 wt.% EC.

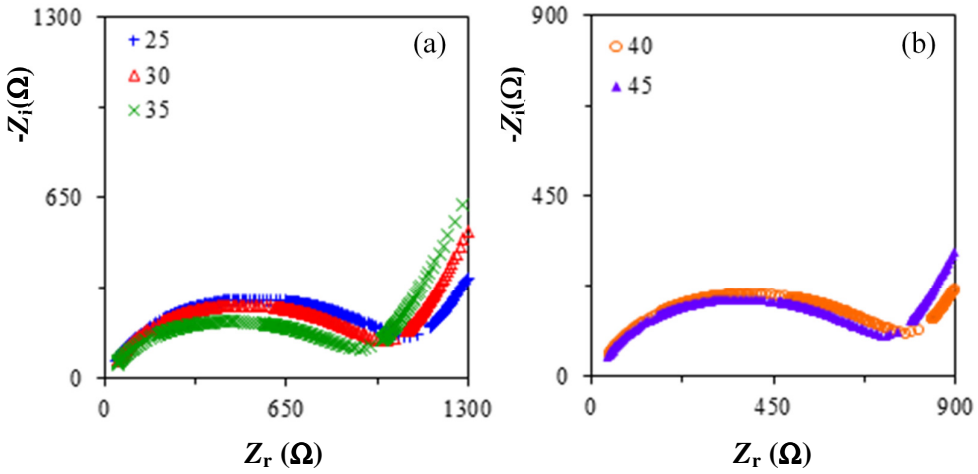

Fig. 7.44. Impedance plot for PCL-NH_4SCN-EC films added with 30 wt.% EC at temperature from 25 to 45 °C.

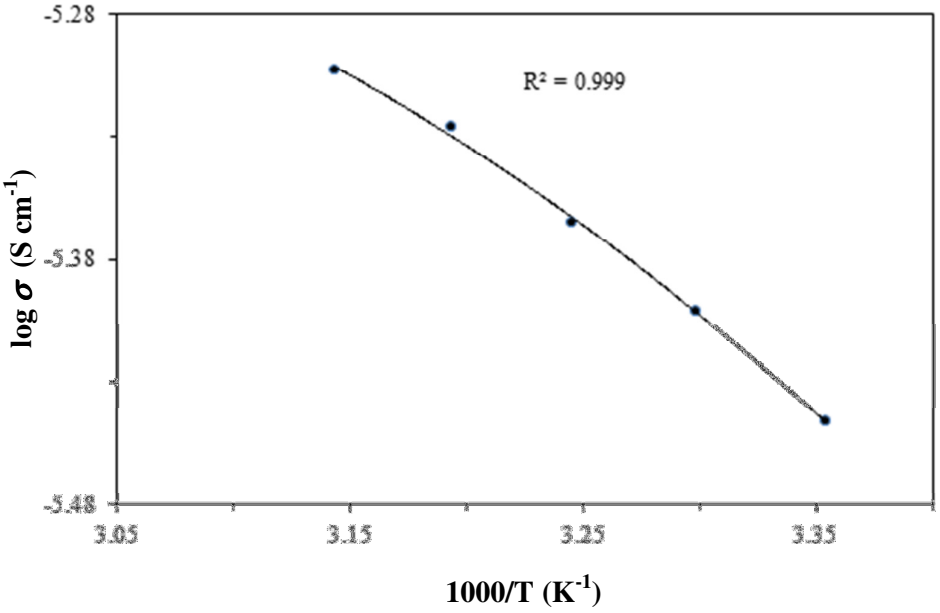

Fig. 7.45. The temperature dependence of conductivity for PCL-NH4SCN-EC films added with 30 wt.% EC.

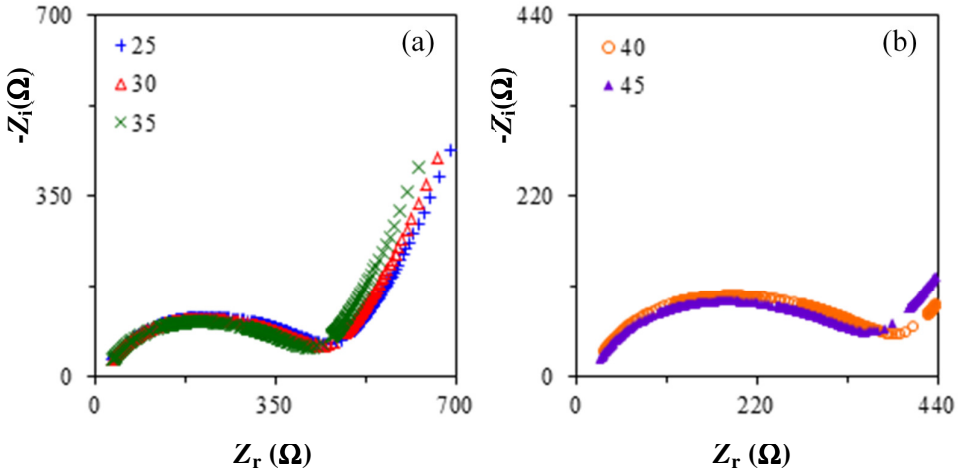

Fig. 7.46. Impedance plot for PCL-NH_4SCN-EC films added with 40 wt.% EC at temperature from 25 to 45 °C.

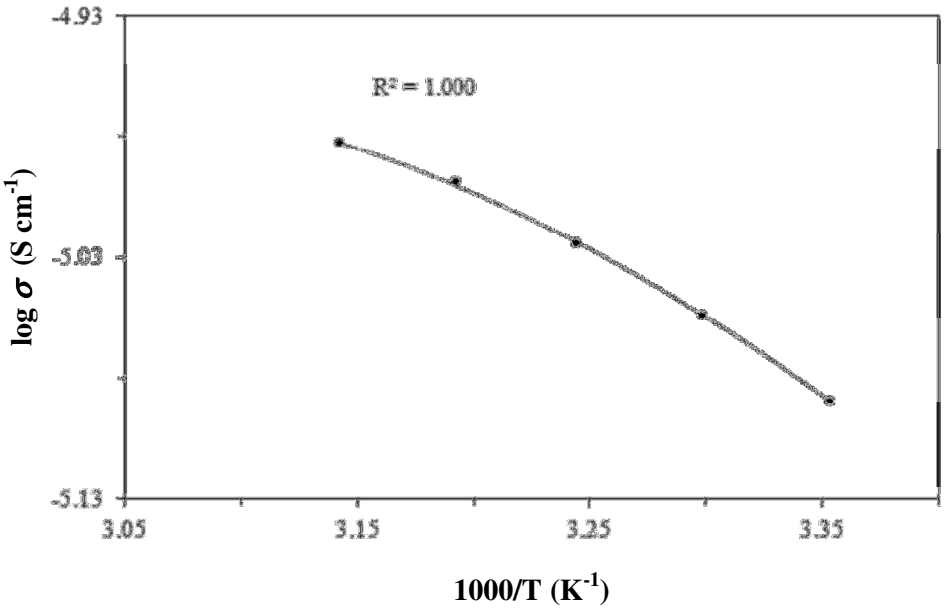

Fig. 7.47. The temperature dependence of conductivity for PCL-NH4SCN-EC films added with 40 wt.% EC.

The linear fit using VTF equation for the temperature dependence conductivity for all PCL-NH_4SCN-EC samples is plotted in Fig. 7.48. T_0 was obtained by trial and error beginning from $(T_g - 50)$ and was subsequently changed to obtain the maximum

regression value. T_g values are obtained from DSC results, in Section 4.3 (Table 4.2). The fitted VTF parameters are displayed in Table 7.2.

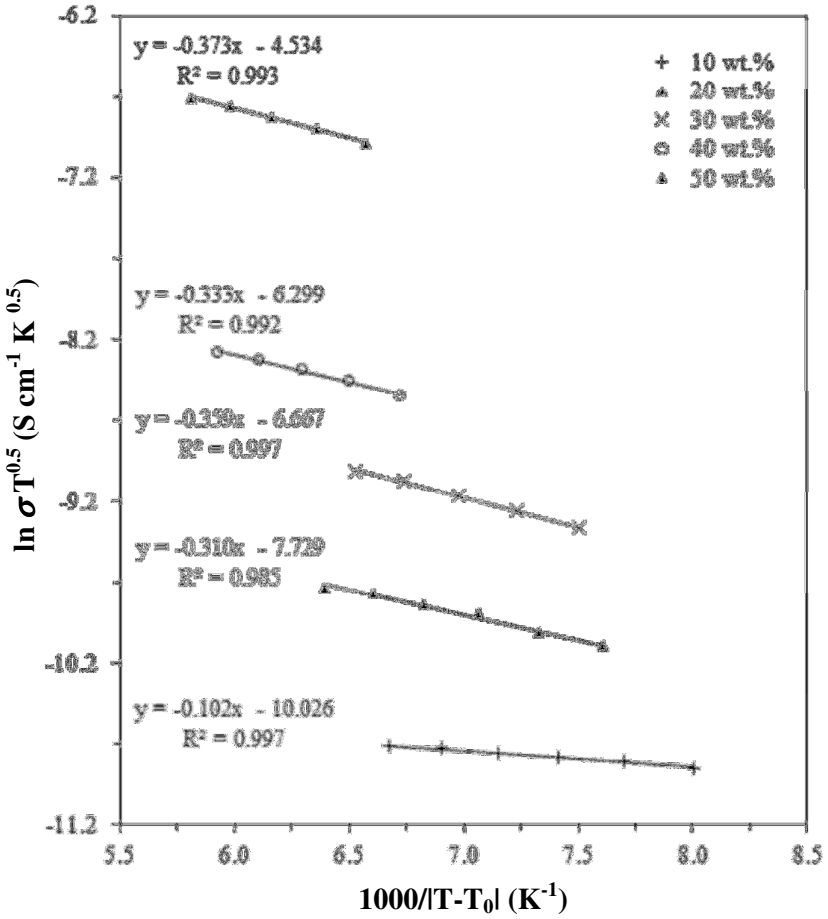

Fig. 7.48. The VTF temperature dependence of conductivity for PCL-NH_4SCN-EC films added with 0 to 50 wt.% EC.

Table 7.2
The VTF fitted parameters from temperature dependence of conductivity for PCL-NH_4SCN-EC films added with 0 to 50 wt.% EC.

EC content, (wt.%)	T_g (K)	R^2	VTF fit			$T_g - T_0$ (K)
			T_0 (K)	A ($S\ m^{-1}\ K^{0.5}$)	B ($x\ 10^3$ K)	
10	213.45	0.997	173.25	4.42×10^{-3}	0.1018	45.5
20	216.25	0.985	166.75	4.40×10^{-2}	0.3101	40.2
30	207.15	0.997	164.85	1.27×10^{-1}	0.3589	49.5
40	196.45	0.992	149.35	1.84×10^{-1}	0.3330	42.3
50	n.a.	0.993	146.00	1.07×10^{0}	0.3734	n.a.

Keynote: n.a. = not available

Fig. 7.48 presents a good fit of conductivity to the VTF equation with regression value of ~0.985-0.997 for all the samples. (T_g - T_0) is calculated to be within the range of 40 to 50 K. This proves that the ionic motion is coupled with the polymer segmental motion. Therefore, the conductivity in PCL-NH_4SCN-EC system is a thermally activated process in which the segmental motion is a determining factor for ionic conduction [Munchow *et al*., 2000].

From Table 7.2, the parameter *A* and *B* are found to increase when more EC is incorporated. A survey on literature shows that similar increasing trend with increasing plasticizer content was reported by Wang and co-workers (2005c). They added two types of plasticizer (EC and PC) separately in their PEO-$LiClO_4$-filler-plasticizer system. Both the value of *A* and *B* is determined to be lower than that in PCL-NH_4SCN system. The fitted value of parameter *B* is in the range of 10^2 K (10^{-2} eV or 1 kJ mol^{-1}). This value is in the same order as PEO-$LiClO_4$-filler-EC system [Wang *et al*., 2005c] with the highest conductivity value of ~10^{-4} Scm^{-1}. Kovac *et al*. (1998) also obtained similar value in PEO-PC-DME-lithium salt system with the highest conductivity value of ~10^{-6} Scm^{-1}.

7.3.4 Temperature Dependence of Dielectric Behavior

A PCL-NH_4SCN-EC sample at 30 wt.% EC is selected for temperature dependent dielectric study. Fig. 7.49 and 7.50 presents the plots of ε' and ε'' as a function of log *f*, respectively, at temperature from 25 to 45 °C.

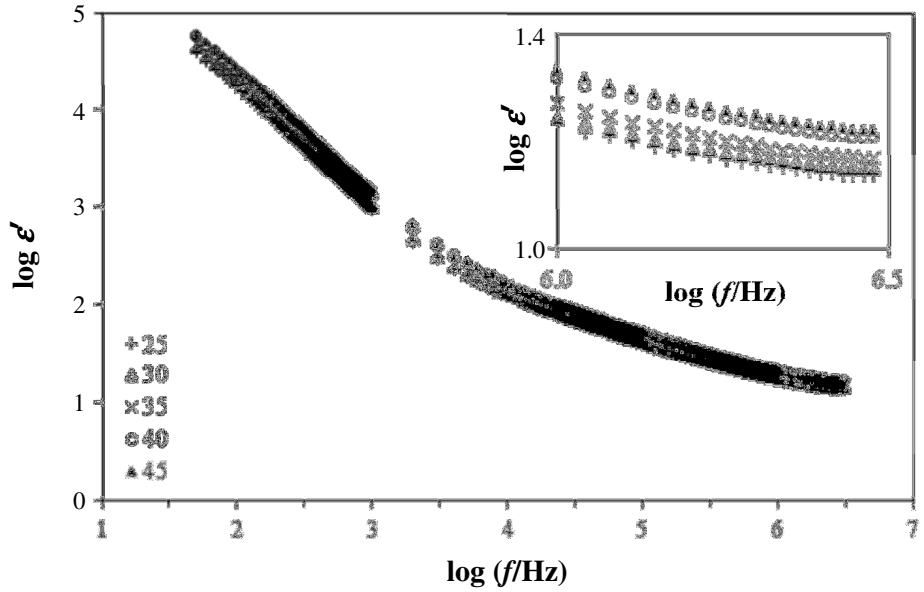

Fig. 7.49. Variation of log ε' versus log f for PCL-NH_4SCN-EC films added with 30 wt.% EC at temperature from 25 to 45 °C. Inset displays the magnified graph.

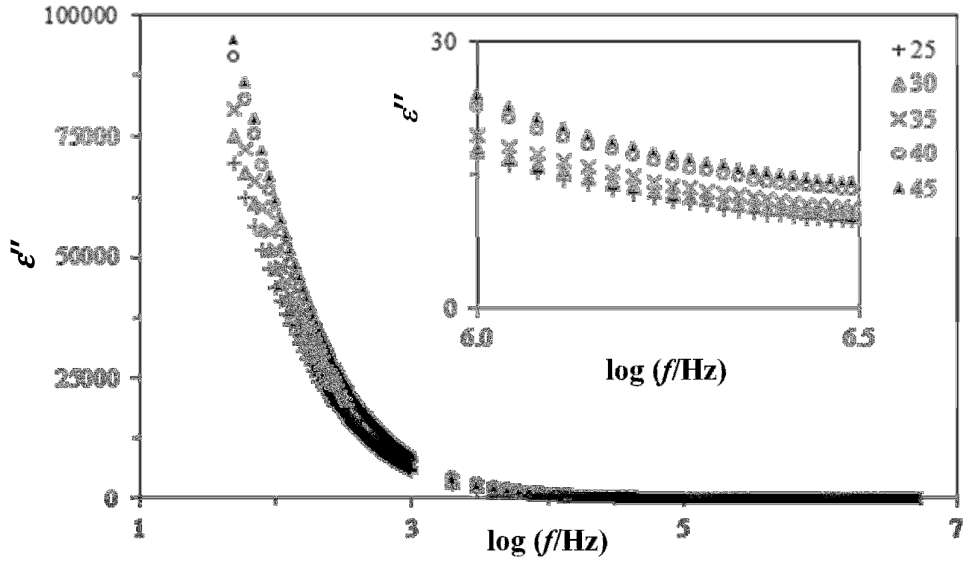

Fig. 7.50. Variation of ε'' versus log f for PCL-NH_4SCN-EC films added with 30 wt.% EC at temperature from 25 to 45 °C. Inset displays the magnified graph.

At low frequency region, both ε' and ε'' show dispersion which is attributed to electrode polarization effect. It can be seen in Fig. 7.49 that ε' increases with increasing

temperature. No relaxation peak of ε'' curve is observed in Fig. 7.50. The electric modulus plots for the same system are illustrated in Fig. 7.51 and 7.52.

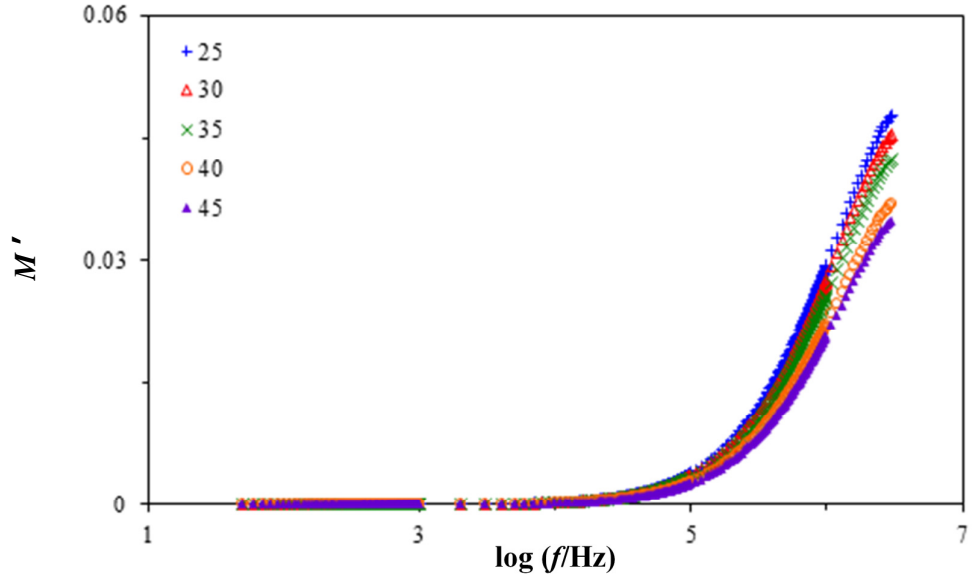

Fig. 7.51. Variation of M' versus log f for PCL-NH_4SCN-EC films added with 30 wt.% EC at temperature from 25 to 45 °C.

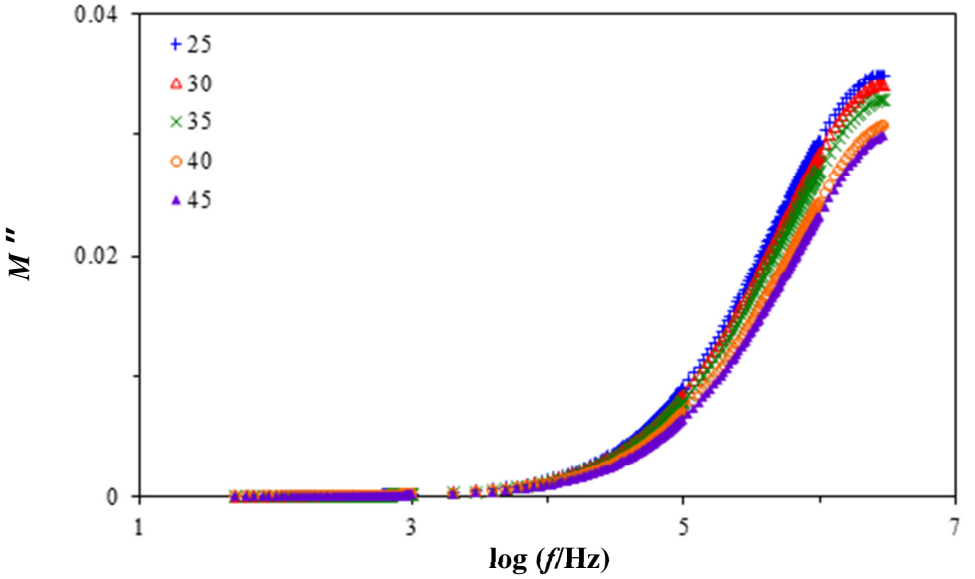

Fig. 7.52. Variation of M'' versus log f for PCL-NH_4SCN-EC films added with 30 wt.% EC at temperature from 25 to 45 °C.

M' versus frequency plot shows the typical sigmoidal curve. At any frequency region, the value of M' shows a declining trend with increasing temperature. This is the opposite observation as in the case of ε'. M'' curve only shows partial dispersion peak where the peak frequency falls outside the frequency window of this work.

Fig. 7.53 presents the variation of loss tangent as a function of frequency at temperature from 25 to 45 °C.

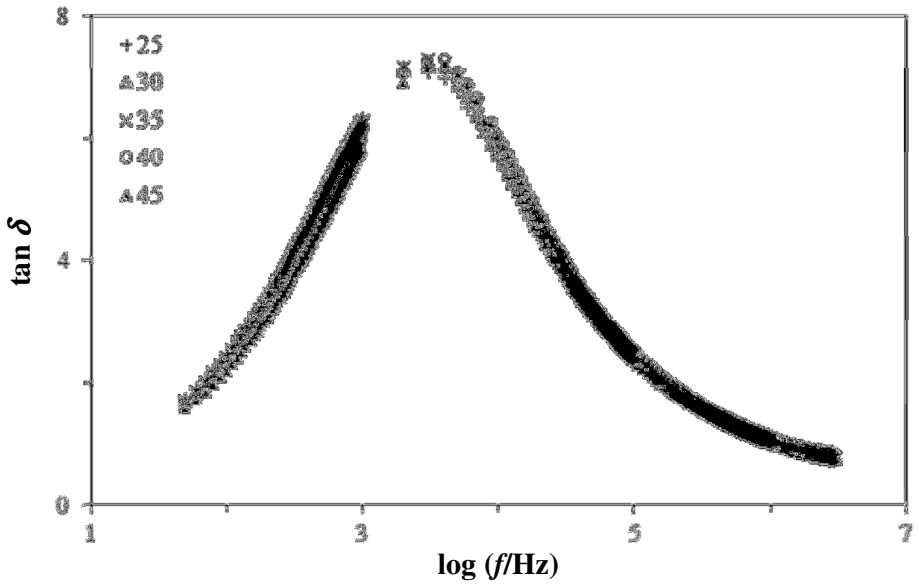

Fig.7.53. Variation of loss tangent versus log *f* for PCL-NH_4SCN-EC films added with 30 wt.% EC at temperature from 25 to 45 °C.

Loss tangent curve shows a single and non-symmetry peak for each temperature. However, the peak is too close to each other for any noticeable shifts. The temperature dependence of the real part of complex conductivity versus log *f* is depicted in Fig.7.54.

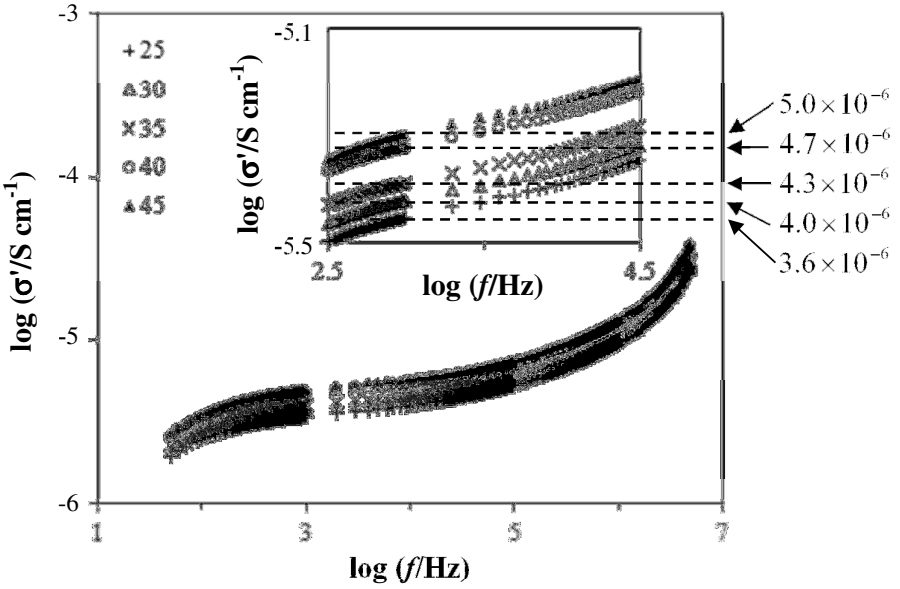

Fig. 7.54. Variation of log σ' versus log *f* for PCL-NH_4SCN-EC films added with 30 wt.% EC at temperature from 25 to 45 °C.

At all temperature range, the graph shows a dispersion at low frequency region, a plateau at middle range frequency and another dispersion at higher frequency region. The plateau is observed to increase consistently as temperature elevates, showing that σ_{dc} is thermally assisted. This plateau can be extrapolated to zero frequency to attain the value of σ_{dc}, which matches the experimental σ_{dc} in Fig.7.46.

7.4 Summary

For PCL-NH_4SCN system:

- Room temperature conductivity of unsalted PCL is obtained as 1.86 x 10^{-10} S cm^{-1}. This value is observed to increase with increasing salt content and reaches

a maximum value of 3.94 x 10^{-7} S cm^{-1} at 26 wt.% NH_4SCN and begin to fall at higher salt content.

- Variation of ε' as a function of salt concentration at room temperature is found to follow the same trend as conductivity study. A strong dependence of conductivity on ε' value is also revealed and this dependence could be contained in the exponential prefactor term, σ_o. From ε' versus log f plot, a dispersion with high value of ε' is observed at low frequency region and ε' decreases rapidly at high frequency region. No appreciable dielectric loss, ε'' peak is observed.

- Single and broad asymmetric M'' peak is observed to shift to higher frequency with increasing salt content up to 26 wt.%. Plot of M'' versus M' clearly shows a depressed semicircle with a center lies below the real axis. These observations deduced the coupling between conductivtiy relaxation and dipolar relaxation.

- From tan δ studies, tan δ peak is observed to shift to higher frequency with the addition of salt concentration up to 26 wt.%, indicating shorter relaxation time. Fig. 7.12 clearly shows that the variation of relaxation time is the inverse of dc conductivity. The estimated σ_{dc} from real part of complex conductivity plot is found to match very well with the experimental σ_{dc} value.

- From temperature dependence of the conductivity study, a good fit to the Vogel-Tamman-Fulcher rule is demonstrated. This concludes the close coupling between the ionic motion and the polymer segmental motion which is in

agreement to the dielectric study. The pre-exponential factor and pseudo energy are found to increase with increasing NH_4SCN concentration.

- From dielectric study, the enhancement in ε' and reduction in relaxation time with elevating temperature shows that polymer segmental motion and ionic motion are thermally activated process.

For PCL-NH_4SCN-EC system:

- Room temperature conductivity of PCL-NH_4SCN-EC film increases monotonically with addition of EC to 3.8×10^{-5} S cm^{-1} at 50 wt.% EC. This indicates that the polymer is capable to contain a large amount of EC molecules.

- Due to the high dielectric constant value of EC (89.8), EC acts as an additive to promote ion dissociation. The fast increasing ε' value at room temperature shows that the number density of free ions is multiplied and lead to further increase in conductivity.

- In M'' versus log f plot, the single and asymmetric peak is found to shift to higher frequency with increasing EC content. The argand plot of M'' versus M' presents a deformed semicircle arc implying the coupling between translational ionic motion and orientational polymer segmental motion.

- From loss tangent study, the variation of relaxation time is found as the inverse of dc conductivity. The estimated σ_{dc} from real part of complex conductivity also matches well the experimental value.

- From temperature dependence of conductivity study, another good fit of conductivity to the VTF equation with regression value of ~0.985-0.997 is obtained for all the samples. This shows that the ionic conduction of this system is the cause of ionic motion coupled with the segmental movement of the polymer chain. The pre-exponential factor increases with increasing EC concentration.

- Dielectric study as a function of temperature presents that the motion of polymer dipoles, salt ions and hence the conductivity are thermally assisted.